Journal of Climate, accepted, 24/04/03

INVERSE ANALYSIS ADJUSTMENT OF THE SOC AIR-SEA FLUX CLIMATOLOGY USING OCEAN HEAT TRANSPORT CONSTRAINTS

Jeremy P. Grist and Simon A. Josey

James Rennell Division for Ocean Circulation and Climate , Southampton Oceanography Centre, Southampton, U.K.

ABSTRACT

Results are presented from a linear inverse analysis of the SOC air-sea flux climatology using ten hydrographic ocean heat transport constraints distributed throughout the Atlantic and North Pacific oceans. A solution is found which results in an adjusted set of fluxes that is consistent with all of the available constraints within their estimated error bounds. The global mean net ocean heat loss to the atmosphere with these adjustments is -5 Wm^{-2}, compared with a gain of 30 Wm^{-2} for the original climatology. The primary changes to the net heat flux arise from an increase of 15 % to the latent heat and reduction of 9 % to the shortwave flux. The analysis has been extended to include the additional constraint that the global mean net heat flux lies in the range 0±2 Wm^{-2}. In the latter case, the solution is modified such that the adjustment of the latent heat increases to 19 %, the reduction of the shortwave decreases to 6 % and the global mean net heat flux is -2 Wm^{-2}. The adjusted SOC fluxes with both solutions agree to within 7 Wm^{-2} with independent large scale area average heat flux estimates obtained from a hydrographic section at 32^{o} S that was withheld from the analysis. Good agreement is also found with recent estimates of the global ocean heat transport obtained using residual techniques and from atmospheric model reanalyses. However, additional comparisons of the adjusted fluxes with measurements made by various Woods Hole Oceanographic Institute research buoys indicate that further improvements to the inverse analysis are still required. Modifications to the analysis scheme are suggested which may lead to further improvements to the adjusted fluxes, in particular the explicit use of the buoy measurements as constraints.

1. INTRODUCTION

In this paper, we present results from a linear inverse analysis of the Southampton Oceanography Centre (SOC) air-sea flux climatology using various hydrographic ocean heat transport constraints distributed throughout the Atlantic and North Pacific oceans. It is well known that climatological estimates of air-sea heat fluxes based on ship meteorological reports have thus far been unable to achieve closure of the global ocean heat budget (e.g. WGASF, 2000). In particular, there is a global mean net heat gain by the ocean of $30 Wm^{-2}$ in the SOC climatology (Josey et al., 1999). Possible reasons for the imbalance include uncertainties in the formulae used to estimate the flux components, as yet uncorrected biases in the meteorological reports and problems due to the limited sampling that is inherent in ship based climatologies (Josey et al., 1999). Resolving the relative contributions from these different effects and developing corrections for them is a difficult problem which is the subject of ongoing research (Josey et al., 2003; Kent, 2002). In the present study, we remove the bias in the SOC climatology through an inverse analysis which employs constraints drawn from the improved picture of spatial variations in the ocean heat transport that has resulted from the World Ocean Circulation Experiment (WOCE). In the longer term we hope to be able to explicitly correct for the various sources of bias and produce a revised version of the SOC climatology which is globally balanced without the need for inverse analysis adjustments.

Our approach follows that of Isemer et al. (1989, IWH hereafter) who were the first to employ linear, discrete inverse theory to refine climatological estimates of the air-sea heat exchange using independent direct estimates of the ocean heat transport from hydrographic sections as constraints. The basic principle of this method is to define various free parameters in the air-sea flux formulae that can be adjusted to achieve improved agreement, in a least squares sense, between the hydrographic heat transport estimates and corresponding values inferred from the climatology. The climatological heat transport estimates are obtained by zonally and meridionally integrating the net surface heat flux with respect to a known transport across a given reference latitude. Our aim is to obtain a balanced set of fluxes which is consistent with the

present hydrographic picture of ocean heat transport by means of physically reasonable adjustments to the different heat flux components.

IWH confined their study to the North Atlantic ocean and considered analyses carried out with various combinations of three heat transport constraints at the equator, 25° N and 32° N. They found that a physically reasonable solution existed when all three constraints were applied provided that the uncertainties in the hydrographic estimates were taken into account. Subsequently, da Silva et al. (1994, dS hereafter) extended this approach to an inverse analysis of a global flux climatology with the additional constraint of zero net heat transport at 65° S. In both analyses, the primary contribution to the constrained net heat flux arose from adjustments to the latent heat flux component. In the period following the dS analysis there has been a significant increase in the number of hydrographic ocean heat transport estimates available for use as constraints, primarily as a result of WOCE. We have taken advantage of this increase and used up to ten heat transport estimates from the Atlantic and North Pacific basins as constraints in our analysis. We will present various inverse method solutions and show that it is possible to obtain adjusted fields of the net heat exchange which formally satisfy all of the hydrographic constraints within their associated error ranges. However, we will also demonstrate that problems remain with regard to obtaining agreement between the adjusted fluxes and local high quality measurements from research buoys which suggest further refinements to the method are necessary in order to produce a fully consistent solution. In particular, we confirm the suggestion of Josey et al. (1999) that inverse analyses with spatially fixed parameter adjustments lead to poorer agreement between the adjusted fluxes and certain key buoy deployments.

As well as providing a set of constraints for the inverse analysis of the SOC climatology, the hydrographic ocean heat transport estimates provide a useful tool for evaluation of other recent climatologies. These include climatologies from atmospheric model reanalyses (NCEP/NCAR and ECMWF) and residual determinations which utilise a combination of reanalysis fields and remotely sensed measurements of the top of the atmosphere radiative flux (Trenberth et al., 2001). A feature of these alternative sources of surface flux estimates is that they have tended to avoid the large global biases inherent in the ship based studies. We have used the available hydrographic heat transport estimates to infer regionally averaged surface heat flux

values and discuss the level of agreement between these values and other available climatologies in the context of the results of our inverse analysis.

The present paper represents an extension of Josey et al. (1999) which detailed the development and evaluation of the original SOC climatology. The structure of the paper is as follows, in the next section we describe the datasets used in our study including a discussion of the difficulties inherent in determining surface flux fields from ship reports and an overview of hydrographic estimates of the ocean heat transport. In Section 3, the inverse analysis method is briefly described with reference to IWH for further details. The results of the analyses are presented in Section 4 together with a comparison of other recent climatologies against hydrography. Finally, we summarise and discuss the implications of our results in Section 5. We note that a more detailed description of the inverse analysis results may be found in Grist and Josey (2002).

2. DATASETS AND CONSTRAINTS

2.1. The SOC Climatology

The primary dataset for our analysis is the SOC climatology which was derived from voluntary observing ship reports in the Comprehensive Ocean - Atmosphere Dataset 1a (Woodruff et al., 1993), covering the period 1980-1993. Additional information regarding observing procedure was merged onto this dataset from the World Meteorological Organisation International List of Selected, Supplementary and Auxiliary Ships (e.g. WMO, 1993) to allow corrections to be made for various biases in the ship meteorological reports (Kent, 1993ab). The method used for the production of the climatology is fully described in Josey et al. (1998).

Significant progress in reducing systematic errors was made during the development of the SOC climatology as a result of the corrections for the ship report biases. These corrections were based on an earlier analysis of a subset of the voluntary observing ship fleet reporting in the North Atlantic for which detailed information regarding observing procedure was available (Kent, 1993ab). The effect of the corrections was found to be complex with changes of up to 15 Wm^{-2} in the monthly mean net heat flux which showed significant regional and seasonal variations. The

regional variations depended primarily on the spatial distribution of different measurement methods and incident solar radiation as well as the magnitude of the flux component being corrected; for a full discussion of the corrections and their effects see Josey et al. (1999).

Estimation of the random errors in ship-based flux fields requires knowledge of the errors in the original meteorological observations, of the strength of the spatial and temporal correlations between the variables in the flux formulae, and of the propagation of errors during the averaging procedure employed (Josey et al., 1999). There are likely to be sampling errors that arise from the non-uniform spatial distribution of ship reports which tend to be concentrated in the Northern Hemisphere ocean basins. The accuracy of the calculated fluxes is thus likely to be considerably reduced in poorly sampled regions such as the Southern Ocean (Josey et al., 1999). Gleckler and Weare (1997) attempted to estimate the errors in the Oberhuber (1988) flux climatology using estimates for the random errors and standard sampling theory. However, Josey et al. (1999) noted difficulties in applying this method to the SOC climatology due to uncertainties over the many meteorological variable and transfer coefficient correlation terms which are required to derive the error fields. Consequently, the main method of evaluation of errors in the SOC fields was a comparison with research buoy measurements; we employ the same technique to evaluate the adjusted fluxes resulting from the present study.

Further discussion of the various sources of sampling and random errors that affect air-sea flux datasets in general, including errors arising from the choice of flux parameterisation, is given at length in the report of the WGASF (2000). One of their main conclusions was that the development of surface flux reference sites (i.e. high quality research buoys of the type deployed by the group at WHOI, e.g. Weller et al., 1998) in several key regions, e.g. the Southern Ocean, would make an important contribution to the quantification of flux errors. We note that the need for such reference sites remains as strong as ever.

It remains the case that all well prepared voluntary observing ship report based flux climatologies have significant heat flux imbalances which average to a gain of order 30 Wm^{-2} in the global mean (da Silva et al., 1994; Josey et al. 1999). Progress is being made towards reducing these biases through the careful development of further corrections for biases in both the ship reports (e.g. Kent, 2002) and the flux formulae (e.g. Josey et al., 2003). However, we are still some way from being able to produce a fully balanced climatology on the basis of improved

corrections alone. Hence, it is timely for us to make use of the additional information provided by the WOCE hydrographic heat transport estimates to constrain the SOC climatology within the framework of an inverse analysis.

2.2 Hydrographic Estimates of the Ocean Heat Transport

The constraints used in the inverse analysis comprise various hydrographic estimates of the ocean heat transport, as well as the optional requirement of global heat budget closure. The heat transport estimates are detailed in Table 1 and the sections employed shown schematically on Fig. 1a together with labels (e.g. AT1) for various regions, bounded by hydrographic sections, that will be referred to later in our discussion. Our choice of constraints is based on the recent review of ocean heat transport estimates by Bryden and Imawaki (2001) and is not intended to be a complete set of all values in the literature but rather a reasonably broad selection of sections undertaken during the period of the SOC climatology. Climatological estimates of the heat transport have been obtained, as detailed in the next section, by integrating the net surface heat flux southwards with respect to high latitude reference transport values which we take from Aagaard and Greisman (1975), these values are also listed in Table 1. Note that subsequent to our analysis Wijffels et al. (2001) have estimated the heat transport across a combined Indo-Pacific section at 32^{o} S to be -0.9±0.29 PW. This value has not been used as a constraint in the inverse analyses discussed here but has been employed for the regional evaluation of the fluxes and the section is also indicated on the figure.

The distribution with time of the various hydrographic sections relative to the period spanned by the SOC climatology is shown in Fig. 1b. The constraints extend over most of the SOC climatology period with a slight increase in numbers towards the end of the interval which reflect the advent of WOCE. It is possible that this distribution might lead to an inverse analysis solution which is biased towards conditions at the end of the period considered. In this context, we note in advance that we have examined solutions in which the number of constraints towards the end of the period has been reduced in order to produce a more even temporal distribution and have found that this has only a minor impact on the required adjustments (see Sec 4.2).

Considerable progress has been made in the determination of the ocean heat transport as a result of WOCE with, for example, widespread use of Acoustic Doppler Current Profile (ADCP)

instruments for improved determination of velocity and current meter arrays, on a number of sections, to obtain accurate measurements of the western boundary currents (Bryden and Imawaki, 2001). However, despite this progress, interpretation of the resulting heat transport values and their associated error estimates is complicated by variations in the computational methods employed between different studies. Bryden and Imawaki (2001) review the main sources of uncertainty which include the selection of reference level velocity for geostrophic calculations, the representation of the heat flux due to eddies and the treatment of the Ekman transport. The interested reader is referred to their review for further details. In addition, Josey et al. (2002) provide a discussion of variations in the Ekman transport that may arise from the choice of wind stress climatology. They highlight the fact that the Hellerman and Rosenstein (1983) climatology is still occasionally being used to obtain estimates of the Ekman contribution to the heat transport despite the weight of observational studies which now clearly show that it overestimates the wind stress, and consequently the Ekman transport, by approximately 25% as a result of the drag coefficient employed. As well as the variations in the method used to estimate the value of the heat transport, there are also differences in the method used to estimate the errors on these values (see Koltermann et al., 1999 for further discussion of error estimation methods). Despite these concerns we have chosen to use the transport values and the associated error estimates as given in the original hydrographic studies as it is not feasible to attempt a revision of these estimates given the detailed understanding of the original datasets that would be required. In this context, we note that the results to be discussed in Sec. 4 show that the solutions obtained with all 10 constraints are able to satisfy each one within its error estimate suggesting that these estimates are not unrealistically small. We note further that improvements to the method used to estimate the ocean heat transport from hydrographic observations (e.g. use of direct ADCP velocity measurements and wind stress fields at the time of the section rather than climatological values) will aid studies such as our own in which these estimates are used to either constrain or evaluate the accuracy of surface flux datasets.

A further source of concern arises from the possible effects of interannual variability in the heat transport which is expected to be more of a problem at some latitudes than others (e.g. Koltermann et al., 1999; Bryden & Imawaki, 2001). The WOCE hydrographic estimates of the heat transport have typically been corrected as far as possible for seasonal effects, particularly variations in the Ekman transport (Bryden & Imawaki, 2001) but remain specific to a particular

year. The only reliable way to quantify the degree of interannual variability is by obtaining repeat hydrography along a given section and such measurements are only available for a very limited number of latitudes. Estimates of the heat transport across 24° N in the Atlantic indicate that there is little interannual variability at this latitude, Lavin et al. (1998) obtain values of 1.27 PW for a section taken in 1957, 1.20 PW in 1981 and 1.33 PW in 1992. Koltermann et al. (1999) obtain a similar lack of variability at 24° N but find much stronger variability from repeat sections at 36° N (0.47 PW in 1957, 1.29 PW in 1981 and 0.70 PW in 1992) and intermediate variability at 48 ° N (0.27 PW in 1957, 0.62 PW in 1981 and 0.53 PW in 1992). However, the accuracy of the estimates at 36° N and 48° N has been called into question by Bryden & Imawaki (2001) primarily on the grounds that the values adopted by Koltermann et al. (1999) for the Gulf Stream transport are far less than observed. Thus, it remains unclear how large the actual variability is at these latitudes.

Apart from 24° N, estimates of the variability based on repeat hydrography are not available for the other sections that we have employed as constraints. Consequently, we have been forced to assume that the reported values are representative of the period covered by the SOC climatology. We note that this period is only 14 years in length so multidecadal variability in the ocean circulation which might cause a problem for analyses of climatological datasets with a longer timebase (e.g. da Silva et al., 1994) is not an issue for our study. Ongoing analysis of the data from WOCE and improvements in the ability of models to adequately represent the ocean heat transport will shed more light on whether our assumption that the chosen constraints are representative is well founded. In this context, we note that the results of our analysis will be shown to be consistent with those of Ganachaud and Wunsch (2001) who have attempted to produce a description of the ocean circulation for the full WOCE period via a model inversion of the hydrographic observations (see Sec 4.1.). Hence, it is unlikely that our results are biased by certain sections being unrepresentative of the mean heat transport within the period considered.

Finally, we note that exchanges with marginal seas have not been taken into account in the analysis as they are generally small in magnitude relative to the heat transport in the larger ocean basins. The net export of heat from the Atlantic to the Mediterranean Sea, which is the largest marginal sea, corresponds to 5 Wm^{-2} heat loss averaged over the Mediterranean basin (Macdonald et al., 1994). However, this is a very small amount in the context of the heat transport in the

Atlantic. The total area of the Mediterranean Sea is approximately 2.5 x 10^{12} m^2 thus the heat input from the Atlantic is about 0.013 PW. This is a negligible amount compared to the total transport in the Atlantic which is of order 1 PW at the latitude of the Mediterranean.

2.3. Comparison Flux Datasets

As noted in the Introduction we have also carried out a regional evaluation of various other recent surface heat flux climatologies. These include a.) atmospheric model reanalysis fluxes from the National Center for Environmental Prediction / National Center for Atmospheric Research (NCEP/NCAR, Kalnay et al., 1996) averaged over the period 1979-1998; b.) reanalysis fluxes from the European Centre for Medium Range Weather Forecasting (ECMWF, Kallberg, 1997) for 1979-1993; c.) residually derived fluxes determined from a combination of NCEP/NCAR output and satellite measurements of the top of the atmosphere radiative flux by Trenberth et al. (2001), for 1985-89, referred to as Trenberth hereafter, and d.) ship meteorological report based fluxes from the University of Wisconsin-Milwaukee / Comprehensive Ocean - Atmosphere Dataset (UWM/COADS) climatology (da Silva et al., 1994), for 1945-1989. Note that Trenberth et al. (2001) have also produced residual estimates using the ECMWF reanalysis instead of NCEP/NCAR but have found that these are less reliable than the NCEP/NCAR derived fields so we have not considered them in the present analysis.

3. THE INVERSE METHOD

In this section we outline the inverse method, our formulation of the problem follows that of IWH who provide a more detailed discussion.

3.1. Single Constraint.

The basic principle of the inverse method as applied here is to adjust various free parameters in the formulae used to estimate the air-sea heat flux in order to obtain better agreement, in a least squares sense, between hydrographic estimates of the ocean heat transport at various latitudes and the corresponding values inferred from the climatology. Consider first an inverse analysis of the climatological fluxes with the single hydrographic constraint that the ocean

heat transport across a given latitude, φ, is $\hat{H}_\varphi$. A climatological estimate, H_φ, of the heat transport may be obtained by integrating the net heat flux, Q_N, across successive latitude bands from a reference latitude φ_o which has a known value of the heat transport, H_o, from hydrography,

$$H_\varphi = H_o - \int_\varphi^{\varphi_o} \int_{\lambda_1}^{\lambda_2} Q_N \, d\lambda \, d\varphi \qquad (1)$$

where λ_1 and λ_2 are the longitude limits at the western and eastern continental boundaries respectively of a given latitude band. The general form for this equation includes a term that accounts for heat storage by the ocean. However, as heat storage is likely to be small over the period covered by the SOC climatology we have made the same assumption that IWH took in their analysis and set the storage term equal to zero. Note that this assumption may not be applicable at shorter interannual timescales when the heat storage term should be explicitly included in the equation. Note also that we adopt a sign convention whereby a positive value for the heat flux implies a gain of heat by the ocean and a positive value for the heat transport signifies northwards flow. The net heat flux is the sum of four components,

$$Q_N = Q_E + Q_H + Q_L + Q_S \qquad (2)$$

where Q_E, is the latent heat; Q_H, the sensible heat; Q_L, the longwave flux and Q_S, the shortwave. The different heat flux components are estimated using various semi-empirical flux formulae.

For the purpose of the analysis we introduce a number, m, of adjustable parameters, p_1, ... , p_m, into the flux formulae; the details of the formulae and parameters are not important at this stage but will be discussed in Sec 3.3. Within the inverse analysis the net heat flux can then be considered to be simply a function of latitude, longitude and the various adjustable parameters, $Q_N(\varphi, \lambda, p_1, ..., p_m)$. The initial values for the parameters are set equal to 1 and are denoted by the superscript *. Estimates of the net heat flux and its components prior to carrying out the inverse analysis adjustment are also denoted by the superscript *, and are referred to as the *original* (or *unconstrained*) estimates. The original climatological estimate of the heat transport across latitude φ may then be written,

$$H^*_\varphi = H_o - \int_\varphi^{\varphi_o} \int_{\lambda_1}^{\lambda_2} Q^*_N(\varphi, \lambda, p^*_1, ..., p^*_m) d\lambda \, d\varphi \qquad (3a)$$

$$= f(\varphi, p^*_1, ..., p^*_m) \qquad (3b)$$

The aim of the inverse method is to modify the values of the free parameters such that an *adjusted* (or *constrained*) climatological estimate of the heat transport may be obtained which equals the hydrographic value, $\hat{H}_\varphi$. Thus, new values $\hat{p}_1, ..., \hat{p}_m$ of the parameters are sought which satisfy the equation,

$$\hat{H}_\varphi - f(\varphi, \hat{p}_1, ..., \hat{p}_m) = 0 \qquad (4)$$

Now for sufficiently small parameter changes, the adjusted heat transport can be expressed as a linear expansion of the original estimate, hence we can write,

$$\hat{H}_\varphi = H^*_\varphi + \sum_{i=1,m} A_i(\hat{p}_i - p^*_i) = H^*_\varphi + \sum_{i=1,m} A_i x_i \qquad (5)$$

Where the term $A_i = \partial H^*_\varphi / \partial p^*_i$ measures the sensitivity of the original climatological heat transport estimate to changes in the various parameters and for convenience we have defined the adjustment to each individual parameter to be $x_i = \hat{p}_i - p^*_i$. Rearranging (5) we have the following linear constraint on the parameter adjustments,

$$\sum_{i=1,m} A_i x_i = \hat{H}_\varphi - H^*_\varphi \qquad (6)$$

IWH discuss both the special case where the heat transport constraint is assumed to be exact and the more general situation where it has a non-zero observational error, $\hat{\sigma}$. For our analysis, all of the hydrographic constraints have associated errors, thus we present here only the equations for the general situation. In that case, equation (6) is solved subject to the least squares condition,

$$\sum_{i=1,m} x_i^2 / e_i^2 + (\hat{H}_\varphi - f(\varphi, \hat{p}_1, ..., \hat{p}_m))^2 / \hat{\sigma}^2 = \text{minimum} \qquad (7)$$

where the e_i are the standard deviations of the p^*_i which are assumed to be normally distributed random variables. The least squares condition follows from a Maximum Likelihood principle

given this assumption (IWH). Using the method of Lagrange multipliers (e.g. Menke, 1984) the following solution for the adjustment to the i^{th} parameter can then be found,

$$x_i = (\hat{H}_\varphi - H^*_\varphi) e_i^2 A_i / (\sigma^{*2} + \hat{\sigma}^2) \tag{8}$$

where the weighting factor,

$$\sigma^{*2} = \sum_{i=1,m} e_i^2 A_i^2 \tag{9}$$

Note that for convenience, the individual parameter adjustments are often combined to form the solution vector $\mathbf{x} = (x_1,...,x_m)$. Regarding the acceptability of different solutions to the analysis, we have adopted the criterion of IWH who discuss the difficulties that arise with formal confidence tests and suggest that the solutions be deemed acceptable if they satisfy the simple consistency check that $|x_i| < e_i$ for all i.

3.2 Multiple Constraints

The method described above may be simply extended, as discussed by IWH, to n > 1 constraints, $\hat{H}_\varphi(j)$ for j = 1,...,n, in which case the solution is,

$$\mathbf{x} = W_e^{-1} A^T \left[A W_e^{-1} A^T + W_\sigma^{-1} \right]^{-1} \mathbf{h} \tag{10}$$

where W_e = diag(e_1^{-2},...,e_m^{-2}) is a square matrix containing the reciprocals of the parameter errors squared; A is an n by m matrix of the sensitivities, with elements,

$$A_{ji} = \partial H^*_{\varphi(j)} / \partial p_i^* \tag{11}$$

; W_σ = diag(σ_1^{-2},..., σ_n^{-2}) is the weighting matrix of the constraint errors and **h** is a vector of dimension n containing the difference ($\hat{H}_\varphi(j) - H^*_\varphi(j)$) between the constraint and the original estimate for each of the n constraints.

3.3. Choice of Adjustable Parameters

We now consider the choice of adjustable parameters (p_1 , ... , p_m) to be used in the inverse analysis. The specification of these parameters is a difficult task and we have investigated a range of values for the parameter errors for the analyses discussed here, our eventual goal being a more detailed specification of the errors based on ongoing research. The assumptions we make are similar to those employed by dS with the primary difference being in the radiative flux terms.

Considering the turbulent (i.e. latent and sensible) heat flux terms first, the original estimates are typically obtained with the well known bulk formulae (see e.g. dS),

$$Q_E^* = \rho L C_e u (q_s - q_a) \qquad (12)$$

$$Q_H^* = \rho c_p C_h u (T_s - T_a) \qquad (13)$$

where ρ is the density of air; c_p, specific heat capacity of air at constant pressure; L, latent heat of vaporisation; C_h and C_e, stability and height dependent transfer coefficients; u, wind speed; T_s, sea surface temperature; T_a, surface air temperature with a correction for the adiabatic lapse rate; q_s, 98% of the saturation specific humidity for pure water at the sea surface temperature, and q_a, atmospheric specific humidity. The factor of 98% allows for the reduction in the saturation specific humidity caused by the salinity of the seawater (e.g. Fairall et al., 1996). For the inverse analysis, dS defined adjustable parameters which were coefficients (p_E and p_H) on the original estimates such that the adjusted flux estimates are as follows,

$$Q_E = p_E Q_E^* \quad ; \quad Q_H = p_H Q_H^* \qquad (14)$$

Note that the original flux estimates (Q_E^*,Q_H^*) which appear in these equations are the individual values obtained for each meteorological report.

dS discussed the difficulties in obtaining accurate estimates of the parameter errors and adopted a value of 0.2 for both e_E and e_H. For their study, IWH employed functionally similar bulk formulae to dS, although the values adopted for the various coefficients in both the turbulent and radiative flux equations were different (see IWH and dS for details of the coefficients employed). The approach taken by IWH to the specification of the inverse analysis parameters differed from dS in that they allowed certain variables in the formulae to vary rather than

explicitly introducing additional parameters. In particular, they assumed that the primary sources of error were the transfer coefficients and the air-sea temperature difference, and assigned errors of 12%, 24% and 0.2° C to C_e, C_h and $T_s - T_a$ respectively. We have chosen to follow the approach of dS and employed adjustable parameters, p_E and p_H, as defined in (14) with $e_E=e_H=0.2$. This remains a reasonable assumption as the individual errors in the transfer coefficients (WGASF, 2000) and meteorological variables (Kent et al., 1999) are each thought to be of order 10%. We have also experimented with various other error assumptions in particular $e_E=e_H=0.1$, and refer to results obtained with the latter scenario where appropriate, noting in advance that it tends to lead to unacceptable solutions.

It should be noted that the parameters as defined here represent the combined error for each flux component arising from the various terms in the flux formulae. Thus, for the latent heat flux, the error represents the combination of the uncertainties in the wind speed, the sea-air humidity difference and the transfer coefficient. It does not represent the error, for example, on the transfer coefficient or wind speed alone. Thus the parameter adjustments obtained with the various solutions presented in the next section cannot be associated with individual terms in the flux formulae as was the case for IWH. Rather, they should be interpreted as reflecting the combined error in the relevant heat flux component. Thus, for example, a solution in which $p_E=0.15$ indicates that a 15% increase in the latent heat flux is required which should be ascribed to the combined errors in the wind speed, sea-air humidity difference and transfer coefficient. It does not indicate that any of the individual terms should be increased by 15% and thus cannot be used as an argument for tuning, for example, the transfer coefficient by this amount.

Note also, that the choice of a fixed 20% (or 10%) error range for these parameters is to a certain extent arbitrary since, as noted in Section 2.1, we expect there to be spatial variations in the magnitude of the total error for each heat flux component arising both as a result of variations in the correlation terms between variables in the flux formulae and because of the uneven distribution of ship reports. The study of Gleckler and Weare (1997) has attempted to quantify this spatial variability for the Oberhuber (1988) climatology. However, as discussed by Josey et al. (1999), we believe that the uncertainty over the correlation terms does not make such an exercise worthwhile at present for the SOC climatology. Hence, for the analysis results presented here we have adopted fixed values for the parameter errors but note that we are currently developing a

more complex analysis scheme which includes a term in the specification of the parameter error which depends on the number of ship observations at a given location.

For the longwave flux, the formula of Clark et al. (1974) which follows was employed in the SOC climatology,

$$Q_L^* = \varepsilon\sigma_{SB} T_s^4 (0.39 - 0.05e^{1/2})(1 - \lambda n^2) + 4\varepsilon\sigma_{SB} T_s^3 (T_s - T_a) \qquad (15a)$$

where ε is the effective emittance of the sea surface, taken to be 0.98 ; σ_{SB}, the Stefan - Boltzmann constant ; e, the water vapour pressure; n, the fractional cloud cover, and λ, a latitude dependent cloud cover coefficient. dS employed a similar formula and introduced adjustable parameters which were associated with the individual water vapour and cloud cover coefficient terms. IWH used the following longwave parameterisation,

$$Q_L^* = \varepsilon\sigma_{SB} T_a^4 (0.254 - 0.00495e)(1 - cn^d) + 4\varepsilon\sigma_{SB} T_a^3 (T_s - T_a) \qquad (15b)$$

where c is again a latitude dependent cloud cover coefficient and the exponent, d, on the fractional cloud cover takes the value 1 (see Isemer and Hasse, 1987 for details). They restricted their selection of adjustable variables in the longwave parameterisation to the exponent, d, which was assumed to have an uncertainty of 0.5.

Recent research by Josey et al. (2003) has shown that estimates obtained with the Clark et al. (1974) formula are commonly in error by of order 10 Wm^{-2}. By comparison, the net longwave flux in the SOC climatology typically lies in the range 40 - 70 Wm^{-2}, hence the cruise results suggest that these estimates may have been in error by up to 20%. With this result in mind we have chosen to have a single adjustable parameter for the longwave, p_L, with error e_L=0.2, which appears as a coefficient on the original formula such that $Q_L = p_L Q_L^*$. We have also experimented with alternative values for e_L and discuss additional solutions obtained with e_L=0.1.

For the shortwave flux, the following formula, with minor variations, which is based on Reed (1977) was used by IWH, dS and in the SOC climatology,

$$Q_S^* = (1-\alpha) Q_c [1 - 0.62\,\bar{n} + 0.0019\,\theta_N] \qquad (16)$$

where α is the sea surface albedo ; Q_c, the clear - sky solar radiation, $\bar{n}$, the monthly mean fractional cloud cover and θ_N, the monthly mean local noon solar elevation. Note that the

shortwave estimates obtained with this formula are monthly mean rather than individual values. Note also that the albedo term was not part of the original Reed (1977) parameterisation which specified the downwelling shortwave flux rather than the net shortwave flux into the ocean from the atmosphere; values for the albedo have typically been taken from Payne (1972). As regards the inverse analysis, dS defined adjustable parameters which were associated with Q_c and the cloud cover coefficient (0.62), assigning 10% errors to each; IWH took a similar approach. Recent work by Tragou et al. (1999) has shown that in regions of high aerosol loading shortwave estimates obtained using Reed (1977) can be biased high by of order 10%. We are currently extending their approach to other regions with the aim of including a spatially dependent error field for the effects that neglect of aerosol loading have had on the original SOC shortwave flux estimates in future analyses. For the present study we have combined the uncertainties into a single adjustable parameter which appears as a coefficient, p_S, on (16), i.e. we write $Q_S = p_S Q_S^*$. Solutions have been obtained with e_S=0.1 and 0.2, those obtained with e_S=0.1 will be shown to require unacceptably high adjustments to the latent heat flux so we focus on the case where e_S=0.2. We are aware that 0.2 is a relatively large value for the shortwave parameter error but note in advance that the inverse analysis solutions obtained with this assumption all have adjustments to the shortwave which are < 0.1. Note that the remarks made earlier regarding the interpretation of the latent and sensible heat flux parameters are also applicable to the longwave and shortwave parameters i.e. they represent the combined error for each flux component arising from the various terms in the flux formulae.

Monthly mean estimates of the fluxes in the SOC climatology are produced from the individual estimates by first averaging the individual values onto a 1^o x 1^o grid to produce raw mean fields (with the exception of the shortwave flux for which the estimate provided by the formula is already a monthly mean). These raw mean fields are then objectively analysed to filter out spatial noise and produce interpolated values for grid points at which there is no data. The objective analysis scheme employs a successive correction method (Cressman, 1959) and is the same as that employed by da Silva et al. (1994); full details of the procedure are given in Josey et al. (1998). The values of the adjustable parameters are not modified by the objective analysis if they are defined to be coefficients on the original flux formulae as is the case in our study (da

Silva et al., 1994). Thus, we can write the original estimate of the net heat flux, Q_N^*, which appears in equation (3a) as follows,

$$Q_N^*(\varphi,\lambda) = p_E^* Q_E^*(\varphi,\lambda) + p_H^* Q_H^*(\varphi,\lambda) + p_L^* Q_L^*(\varphi,\lambda) + p_S^* Q_S^*(\varphi,\lambda) \qquad (17)$$

where the various $Q_x^*(\varphi,\lambda)$ terms are the original SOC climatology annual mean values for each of the heat flux components at a given latitude and longitude. The elements of the sensitivity matrix, A_{ji} , may then be obtained by substituting equation (3a) into (11). For example for the term associated with p_E, we find,

$$A_{jE} = \partial H^*_{\varphi(j)} / \partial p_E^* = -\int_{\varphi_j}^{\varphi_o}\int_{\lambda_1}^{\lambda_2} \partial Q_N^*(\varphi,\lambda)/\partial p_E^* \, d\lambda \, d\varphi \qquad (18a)$$

$$= -\int_{\varphi_j}^{\varphi_o}\int_{\lambda_1}^{\lambda_2} Q_E^*(\varphi,\lambda) \, d\lambda \, d\varphi \qquad (18b)$$

The other terms follow in a similar manner resulting in the following elements of the sensitivity matrix,

$$\begin{aligned} A_{jE} &= -\int_{\varphi_j}^{\varphi_o}\int_{\lambda_1}^{\lambda_2} Q_E^*(\varphi,\lambda)\, d\lambda\, d\varphi, \quad A_{jH=} -\int_{\varphi_j}^{\varphi_o}\int_{\lambda_1}^{\lambda_2} Q_H^*(\varphi,\lambda) d\lambda\, d\varphi, \\ A_{jS} &= -\int_{\varphi_j}^{\varphi_o}\int_{\lambda_1}^{\lambda_2} Q_S^*(\varphi,\lambda)\, d\lambda\, d\varphi, \quad A_{jL} = -\int_{\varphi_j}^{\varphi_o}\int_{\lambda_1}^{\lambda_2} Q_L^*(\varphi,\lambda) d\lambda\, d\varphi \end{aligned} \qquad (19)$$

By evaluating these integrals for each constraint and substituting the resulting values into (10), the inverse analysis solution for a given set of parameter errors may then be easily determined.

.

4. RESULTS

In this section, we present solutions from a range of inverse analysis calculations and compare the resulting adjusted SOC heat flux fields with research buoy measurements and various

recent climatologies. Our primary focus will be on results obtained with $e_E=e_H=e_L=e_S=0.2$, however we will also discuss solutions obtained with $e_E=e_H=0.1$, $e_L=e_S=0.2$ and $e_E=e_H=e_L=e_S=0.1$.

4.1. Solutions Without Requirement of Global Heat Budget Closure

a.) Full Set of Constraints

We begin by considering the results of analyses carried out using the heat transport constraints alone without the explicit requirement of global heat budget closure. Values for the parameter adjustments obtained in this case from the inverse analysis with all ten heat transport constraints are listed in Table 2. The main change is to the latent heat flux ($x_E=0.15$) with smaller adjustments to the other terms ($x_S=-0.09$, $x_L=0.09$, $x_H=0.06$). Note that these adjustments are broadly similar to those found by dS who obtained a range of solutions in which the increase to the latent heat flux was in the range 13-17% and the reduction to the shortwave 7-8%. The parameter changes, which we refer to hereafter as Solution 1, have been applied to the original SOC heat flux components and their impact on the global mean heat flux calculated, see Table 3. As a result of the adjustments the global mean net heat flux is reduced from 30 Wm^{-2} to -5 Wm^{-2} i.e. the adjusted fields are significantly closer to achieving closure of the ocean heat budget although they now exhibit a small net heat loss to the atmosphere rather than a strong gain. This change is brought about primarily by a reduction of 16 Wm^{-2} to the shortwave gain and an increase of 14 Wm^{-2} in the latent heat loss with smaller contributions from the other two terms.

The unadjusted net heat flux field from the SOC climatology is shown together with the adjusted field obtained with Solution 1 in Fig.2, their difference is shown in Fig.3. Regions of net heat loss to the atmosphere are largely confined to the western boundary currents and high latitudes in the original SOC field, these being areas where strong air-sea temperature and humidity differences give rise to significant sensible and latent heat fluxes. In the adjusted field, there is a significant expansion of the areas in which net heat loss occurs with a general equatorwards migration of the boundary between net heat loss and gain. The difference plot, Fig.3a, shows the spatial distribution of the changes more clearly, with the largest adjustments, which are in the range 40-50 Wm^{-2}, occurring in the Tropics and boundary current regions. Decomposition of the adjusted net heat flux field into its components, discussed in detail in Grist

and Josey (2002), reveals that the major changes are to the shortwave in the Tropics and latent heat flux at mid-high latitudes.

The climatologically implied ocean heat transports in the Atlantic and Pacific Ocean basins from the original and adjusted SOC fields are shown in Fig.4 together with the hydrographic constraints. Note that the variation shown for the Pacific Ocean is limited to the region north of the Equator as the uncertainty over the magnitude of the Indonesian Throughflow does not allow useful climatological estimates of the heat transport to be obtained for the South Pacific. The transport curves for the unadjusted SOC climatology diverge rapidly from the hydrographic estimates as a result of the strong heat flux bias. For the Solution 1 adjusted SOC fluxes, reasonable agreement across the full range of transport estimates is obtained i.e. there are no outlying values which could not be satisfied within their error limits by this solution. The adjusted fluxes have been checked for consistency with the recent large scale area averaged air-sea heat exchange estimates of Ganachaud and Wunsch (2000, GW hereafter), see Table 4. The GW values were obtained using WOCE section measurements of temperature and salinity that were adjusted in a box model in order to obtain a geostrophic velocity field which allows a range of conservation laws (mass, salt, heat etc.) to be satisfied. The GW values cannot be regarded as being independent from the adjusted SOC fields as there is some overlap in the observations used to formulate the constraints in each case. However, they do allow a test to be carried out of whether the adjusted SOC fluxes are consistent with a box model solution in which mass and salt conservation laws are applied as well as closure of the heat budget. The Solution 1 fluxes are consistent with the GW estimates for each of the latitude bands considered, agreeing to between 1 and 6 Wm^{-2}, while the original SOC fluxes differ by between 20 and 37 Wm^{-2}.

Further comparisons have been carried out between area averaged net heat flux values determined from hydrography and corresponding values from the original and adjusted SOC fields. Hydrographic values have been determined by calculating the difference between the heat transport estimates at the northern and southern limits of each labelled region in Fig. 1 and dividing by the area. In addition to the flux estimates determined from the hydrographic constraints used in the analysis, values have also been obtained for regions IP1 and SO1 using the independent heat transport estimate of -0.90±0.29 PW across 32^{o} S in the combined Indo-Pacific basin from Wijffels et al. (2001). The difference for each region between the area averaged net

heat flux values from climatology and hydrography are shown schematically in Fig.5. We expect reasonable agreement between the adjusted and hydrographic values for those regions that were bounded by constraints used in the analysis. However, the IP1 and SO1 regions provide a test of whether the adjustments have lead to improved flux estimates elsewhere. The unconstrained SOC climatology tends to be positively biased with respect to the hydrographic values by between 20 and 50 Wm^{-2}, see Fig. 5a, the exception being the mid-high latitude North Pacific region PA1 which agrees with hydrography to within 1 Wm^{-2}. As noted by Josey et al. (1999) the strongest biases are in the region of the North Atlantic (AT2) containing the Gulf Stream, for which the difference is 49 Wm^{-2}. Following the Solution 1 adjustments, the area averaged fluxes for each region (Fig.5b) are typically within 20 Wm^{-2} of the hydrographic values. The bias in the AT2 region has been reduced from 49 to 16 Wm^{-2}, however the flux estimate for PA1 now overestimates the heat loss relative to hydrography by 20 Wm^{-2}. For the regions adjacent to the 32° S line the inverse analysis has resulted in encouraging improvements with agreement between the adjusted fluxes and hydrography to within 7 Wm^{-2}. Although no individual region stands out as being strongly biased, it remains the case that there are area averaged biases of ± 20 Wm^{-2} in the fluxes after the inverse calculation which points to the need for further refinements to the analysis as formulated here.

The results described above have all been obtained with $e_E=e_H=e_L=e_S=0.2$. We have also obtained results for other combinations of parameter errors but find that in each case considered the parameter adjustments are larger than the specified error range. Here, we briefly summarise two solutions obtained with more optimistic assumptions for the parameter errors; note that all ten constraints have again been employed. First, we consider the case where the radiative fluxes have smaller errors than the turbulent terms by setting $e_L=e_S=0.1$ while retaining $e_E=e_H=0.2$. With these assumptions, we find that $x_E=0.23$, i.e. the adjustment to the latent heat flux is greater than the prescribed error, although the other terms remain in range ($x_S=-0.06$, $x_L=0.04$, $x_H=0.06$). In the second case we assume that the error on all four terms is only 10% i.e. $e_E=e_H=e_L=e_S=0.1$. We then obtain a solution in which the shortwave adjustment exceeds the prescribed error, $x_S=-0.13$, while the other three values remain in range ($x_E=0.09$, $x_L=0.06$, $x_H=0.02$). Thus, of the 3 combinations considered, only the solution obtained with the assumption of a 20% error for all of the parameters satisfies the self-consistency criterion proposed by IWH. As regards closure of the ocean heat budget, we note that the adjusted SOC global mean net heat flux obtained from the

two alternative sets of adjustments is -4 Wm^{-2} in each case, which is very close to the value of -5 Wm^{-2} found with Solution 1. The problem of obtaining improved heat budget closure is addressed further in Section 4.2.

b.) Solutions Obtained with a Limited Number of Constraints

We have also investigated at length the effects of varying the number of constraints used in the inverse analysis solution. The principal results of this investigation are summarised here, for a more detailed discussion see Grist and Josey (2002). The main result is that when a large proportion (> about 6) of the available 10 constraints are used in the analysis, the parameter adjustments vary little from one solution to another (this point will be illustrated in Sec 4.2. using various 8 constraint solutions). However, when only a limited number of constraints are employed we have found that there is the potential for large variations in the parameter adjustments between solutions as certain regions, e.g. the box containing the Gulf Stream, with strong biases can dominate the analysis.

We demonstrate that this is the case with an example solution in which only the first three sections (CONVEX, 24° N and 14° N) listed in Table 1 are used to provide heat transport constraints for the analysis. The first two of these constraints span the Gulf Stream region which as noted earlier was strongly biased in the unadjusted SOC climatology, the net heat loss being underestimated by 49 Wm^{-2} with respect to the value obtained from hydrography. The solution obtained with the three constraints is as follows: (x_E=0.11, x_S=-0.18, x_L=0.07, x_H=0.02). The main difference between this solution and the 10 constraint case discussed in the preceding section is the sharp increase in the shortwave flux reduction from 9% to 18%. When the 3 constraint solution parameter adjustments are applied to the original SOC fluxes, the bias in the Gulf Stream region falls to 6 Wm^{-2}, so the solution is satisfactory in that respect. However, the globally averaged net heat flux after the adjustment is reduced to -16 Wm^{-2} which is clearly unacceptably low.

Similar problems can arise when only a single constraint is employed and we illustrate that this is the case with two example solutions for 24° N and CONVEX in the North Atlantic. First, if the heat transport estimate of 1.20 ± 0.26 PW at 24° N from Table 1 is employed as the sole constraint on the analysis the same solution (x_E=0.11, x_S=-0.18, x_L=0.07, x_H=0.02) to that found for the 3 constraint case above is obtained. With these adjustments the climatologically implied

heat transport at 24° N becomes 0.94 PW which is just within the error on the hydrographic estimate. However, the global mean net heat flux following the adjustments is again -16 Wm^{-2} i.e. unacceptably strong cooling. In contrast, if the hydrographic heat transport estimate of 0.28 ± 0.06 PW across the CONVEX line is employed as a single constraint the following solution results (x_E=0.07, x_S=-0.11, x_L=0.06, x_H=0.02). In this case the shortwave adjustment is reduced to 11%, the adjusted heat transport across the section is 0.23 PW, which is in agreement with the hydrographic value, and the solution has a global mean net heat flux of 1 Wm^{-2}. The solution obtained using the CONVEX heat transport estimate as a single constraint is therefore more reasonable than that obtained using 24° N alone as it is very close to achieving global ocean heat budget closure. The 24° N and CONVEX results thus demonstrate that there may be significant variations between the quality of different single constraint solutions when they are judged in terms of their ability to produce global heat budget closure.

The examples cited above provide a clear warning that analyses carried out with only a small number of constraints have the potential to produce globally biased solutions. As our goal is to obtain an improved set of global fields, the focus in the remainder of the paper is on solutions in which the full set of 10 constraints has been used in order to avoid particular regions dominating.

4.2 Solutions With Requirement of Global Heat Budget Closure

The globally averaged net heat flux of -5 Wm^{-2} obtained with Solution 1 remains too large to be consistent with the magnitude of observed ocean temperature variations at decadal timescales. Precise estimates of the temperature variations on these timescales are difficult to obtain given the sparseness of repeat hydrographic observations along the same section. However, as an example, repeat hydrography at 24° N in the Atlantic has revealed temperature variations of about 0.2° C to a depth of approximately 1000m between sections taken in 1981 and 1992 (Bryden et al., 1996). For comparison, a bias of 1 Wm^{-2} maintained over the period of the climatology would if mixed into the upper 1000m of the ocean lead to a mean temperature change of that layer by 0.1° C (Josey et al., 1999). This suggests that the global heat budget should close to within about 2 Wm^{-2} in order to be consistent with observations. Although this value has been obtained from only a single repeat section it provides an indicative estimate of the

amount to which the SOC climatology heat budget should be closed. More accurate estimates will become possible as other repeat sections collected during WOCE are analysed.

In order to achieve a global balance with the adjusted SOC fields, we have also obtained solutions in which heat budget closure is included explicitly as one of the constraints on the analysis. We first discuss results from the problem where the heat budget closure is required to be exact, i.e. the global mean net heat flux must exactly equal 0 Wm^{-2}. We then consider the effects of allowing a small error on this constraint and require instead that the mean heat flux equals 0±2 Wm^{-2}, which is consistent with the estimate obtained above. In both cases we present solutions obtained with all 10 heat transport constraints.

Values for the parameter adjustments are listed in Table 2 and their impact on the global mean net heat flux in Table 3. For the case of exact closure, referred to as Solution 2, there is a sharp increase in the latent heat flux adjustment (x_E=0.25) and reduction in the shortwave adjustment (x_S=-0.02) relative to Solution 1. Closure of the heat budget is achieved almost entirely through an increase of 22 Wm^{-2} in the latent heat loss, with only a small reduction, 3 Wm^{-2}, to the shortwave gain. Thus, the requirement of exact closure has resulted in an extreme solution in which the major change is to the latent heat flux field and the magnitude of this change exceeds the prescribed parameter error range i.e. Solution 2 does not satisfy the IWH criterion. Given these results we have relaxed the global mean heat flux constraint by an amount, 2 Wm^{-2}, which is approximately consistent with observations as discussed above, in an attempt to find a solution which satisfies the IWH criterion and is close to closure. In this case we obtain a less extreme set of adjustments (x_E=0.19, x_S=-0.06, x_L=0.09, x_H=0.07), which we refer to as Solution 3. The adjusted global mean net heat flux is now -2 Wm^{-2} as a result of an increase in the latent heat loss of 17 Wm^{-2} and reduction to the shortwave gain of 10 Wm^{-2} with smaller changes to the other two terms. Each of the parameter adjustments now lies within the prescribed error range although the value for x_E is close to the specified limit.

The net heat flux fields obtained when the Solution 2 and 3 adjustments are applied to the SOC climatology are shown in Fig.2 with difference fields in Fig.3. The Solution 2 net heat flux field is broadly similar to that obtained with Solution 1 as regards the boundary between regions of net heat gain and loss. There are however significant differences in the Tropics, where the maximum net heat gain is closer to that found for the original climatology. In addition, for the

boundary current regions the net heat loss adjustment is significantly stronger, approaching 60 Wm^{-2} over both the Gulf Stream and Kuroshio, with Solution 2 than with Solution 1 (compare Figs 3a and b). These differences are to be expected given the extreme adjustments to the latent heat flux in Solution 2 which result in greater changes in these regions (see Grist and Josey, 2002 for details). The net heat gain for Solution 3 has an adjustment pattern (Fig. 3c) which is intermediate between that obtained with Solutions 1 and 2, with significant changes in both the Tropics and boundary current regions.

The implied ocean heat transport in the Atlantic and Pacific is broadly similar for all three solutions, Fig.4ab. However, the differences between the solutions become significant for the implied global ocean heat transport which is shown in Fig.4c together with several hydrographic estimates which were obtained by combining values at the same latitude in different basins, see Table 5. Agreement with the Northern Hemisphere global heat transport estimates is obtained for all of the solutions. In the Southern Hemisphere, Solution 3 is in good agreement with the 32° S value but the other two solutions lie just outside the hydrographic error range for the transport at this latitude. The close correspondence between the climatological and hydrographic estimates of the transport at 32° S indicates that Solution 3 provides an adjusted set of fluxes which remains consistent with hydrography when integrated over a broad latitude range. Note that for Solution 3 there is a small implied heat transport at the Southern boundary of 0.6 PW which corresponds to the global mean net heat flux of -2 Wm^{-2}. As discussed above an imbalance of this amount is consistent with observed decadal temperature variations. Regarding the comparison with the GW flux estimates (Table 4), Solutions 2 and 3 exhibit a similar close level of agreement to that found for Solution 1, the differences being less than 4 Wm^{-2}. Area averaged fluxes obtained from the SOC climatology with the Solution 2 and 3 adjustments are compared with hydrography in Fig. 5. Agreement with the hydrography to within ± 20 Wm^{-2} is again typical with no regions standing out as having biases stronger than about 20 Wm^{-2}.

It was noted in Sec 2.2. that there was a slight imbalance in the temporal distribution of constraints used for our analysis with more towards the end of the period of the SOC climatology because of the advent of WOCE. We have investigated whether this is likely to have had a significant impact on our analysis by obtaining solutions, with the requirement of global closure to within 2 Wm^{-2}, in which some of the constraints are removed and comparing with the

corresponding Solution 3 results obtained with all 10 constraints. In particular, the Atlantic 8° N and 14° N constraints and the 30° S and A11 sections were occupied at approximately the same time (see Fig. 1b) and we have obtained 8 constraint solutions in which one of each of these pairs of constraints has been selectively removed. Very similar results are obtained to those found for the full 10 constraint Solution 3 case. Two examples are given here, for the first the Atlantic 14° N and A11 constraints are removed from the analysis and the solution becomes (x_E=0.17, x_S=-0.07, x_L=0.08, x_H=0.07). For the second, the Atlantic 8° N and 30° S constraints are removed and the solution becomes (x_E=0.18, x_S=-0.07, x_L=0.09, x_H=0.07). Similar results are obtained for the other two possible combinations i.e. removing 14° N and 30° S , and 8° N and A11. In all four cases the solutions differ by only 1-2% in the magnitude of the adjustments relative to the full 10 constraint Solution 3 which suggests that our analysis has not been compromised by having slightly more constraints towards the end of the period considered than the beginning. These results also demonstrate, as noted earlier, that when a large proportion of the available 10 constraints are used, the parameter adjustments vary little from one solution to another.

Finally, in this section, we note that the ten constraint results described above have again been obtained with e_E=e_H=e_L=e_S=0.2 and that various other parameter error combinations have also been investigated with similar results to those described in Sec 4.1 i.e. the parameter adjustment for at least one term is larger than the specified error range. To demonstrate this we briefly summarise two solutions obtained for the 0±2 Wm^{-2} global heat flux constraint case. With e_L=e_S=0.1, e_E=e_H=0.2, we find that x_E=0.25 - i.e. the adjustment to the latent heat flux is again greater than the prescribed error - while the other terms are still in range (x_S=-0.05, x_L=0.03, x_H=0.08). For e_E=e_H=e_L=e_S=0.1, it is the shortwave adjustment that exceeds the prescribed error, x_S=-0.12, while the other three values remain consistent (x_E=0.10, x_L=0.05, x_H=0.03). Thus, of the three error combinations considered, we have again found that only the solution obtained with the assumption of a 20% error for all of the parameters satisfies the self-consistency criterion proposed by IWH.

4.3 Comparison with Independent Research Buoy Measurements

In addition to the large scale constraints provided by ocean heat transport estimates from hydrographic sections, research buoy measurements provide a valuable source of information

which can be used for local evaluation of surface fluxes. We have compared the fluxes obtained by adjusting the SOC climatology according to the different inverse analysis solutions with independent measurements from various Woods Hole Oceanographic Institute (WHOI) research buoys (e.g. Moyer and Weller, 1997). The approach followed is the same as that used for the evaluation of the original SOC fluxes and subsequently the NCEP/NCAR and ECMWF reanalyses (Josey et al., 1999; Josey 2001). The adjusted fluxes at the location of each buoy are compared with the buoy measurements for the period of each deployment. Uncertainties arise from inexact co-location in space and time of the buoy measurements and the ship observations used for the SOC fluxes, and from errors in the buoy measurements. However these tend to be minor terms and the buoy measurements provide a useful reference dataset for evaluation of the fluxes. For full details of the buoys, which were deployed in the North Atlantic, Tropical Pacific Warm Pool and Arabian Sea, and the comparison method and sources of error see Josey et al. (1999). Good agreement between the unconstrained SOC fluxes and the Subduction buoy measurements was found in the earlier study. Consequently, one of the conclusions of that study, which we aim to check, was that adjustment of the SOC climatology through inverse analysis with globally constant changes to the free parameters, as considered here, would cause the adjusted flux estimates to diverge from the buoy values for the Subduction region.

Results of the buoy comparisons are presented in detail for Solution 3, broadly similar results are obtained when the other solutions are considered. Deployment mean values of the heat fluxes measured by the buoy and determined from the original and adjusted SOC datasets are listed in Table 6a-d. Note that the values listed for the Subduction buoy deployment are an array average as described in Josey (2001). The amounts by which the original and adjusted fluxes differ from the research buoy values are shown in Fig. 6. Adjustment of the SOC latent and shortwave flux estimates leads to significantly poorer agreement with the buoy measurements for both the Subduction Array and Arabian Sea deployments. Consequently, the SOC-buoy net heat flux difference for the Subduction Array after adjustment is -45 Wm^{-2} compared to -8 Wm^{-2} before, which supports the conclusion of Josey et al. (1999) noted above. The magnitude of the SOC-buoy difference at the Arabian Sea site also increases after the adjustments although the change is not as dramatic as at the Subduction Array. In contrast, at the TOGA-COARE site, the adjusted shortwave flux is in better agreement with the buoy value, while the latent heat flux is again worse. The original SOC estimate of the net heat flux for the TOGA buoy deployment was

44 Wm^{-2}, significantly higher than the buoy value of 21 Wm^{-2}, while the adjusted value is 8 Wm^{-2} i.e. the adjustment has lead to slightly better agreement. Note that in all three cases the inverse analysis leads to an increase in the net longwave loss which results in better agreement with the buoy measurements of this component. This result is consistent with a recent analysis of longwave measurements (Josey et al., 2002), noted in Sec 3.3, which suggests that the Clark et al. (1974) formula used in the SOC climatology underestimates the longwave loss. Finally, at the FASINEX deployment site (which was at the southern margin of the region of intense heat loss associated with the Gulf Stream) the adjusted latent heat flux is in significantly better agreement with the buoy value although still underestimating the heat loss by 21 Wm^{-2}. This suggests that the adjustment to this component should have been stronger in this region. Unfortunately, there is no estimate of the longwave flux for the FASINEX buoy. However, if one considers the SOC-buoy difference for the sum of the other three components as being indicative of that for the net heat flux, then the adjustment has produced a significant improvement as this difference is 50 Wm^{-2} before the adjustment and 13 Wm^{-2} afterwards.

In summary, the results of the buoy comparisons are mixed, there is improved agreement of the adjusted fluxes with the buoy measurements for TOGA-COARE and FASINEX but poorer agreement for the Subduction Array and Arabian Sea buoys. The results provides a warning that significant local biases remain in the adjusted fluxes, even though improved agreement has been obtained regionally with hydrography. They suggest that improvements can be made to the inverse analysis for example through the direct use of the buoy measurements as constraints and we plan to investigate this possibility in future work.

4.4. Comparison with Other Recent Climatologies

In this section, we discuss the results of the inverse analysis in the context of the various other recent flux climatologies (NCEP/NCAR, ECMWF, UWM/COADS and Trenberth) which were detailed in Section 2. Climatological annual mean net heat flux fields for each of these datasets are shown in Fig. 7. The principal features of the heat exchange fields i.e. strong losses in the boundary current regions and gains in the Tropics, particularly the eastern equatorial Pacific, are the same in each case. However, significant differences between the fields do exist, in particular the Trenberth residual method climatology shows more extreme heat loss and gain over the

boundary currents and Tropics respectively than the other datasets. This tendency is highlighted when zonal averages of the fields are taken, Fig. 8. The residually derived fluxes have a mean heat gain on the Equator of 75 Wm^{-2} while the other analyses tend to cluster around 50 Wm^{-2}. Likewise, in the 35-40^{o} N band that contains the Kuroshio and Gulf Stream, the strongest zonal mean losses are those for the Trenberth fluxes. By comparison, the Solution 3 zonal mean variation tends to lie in the in middle of the range defined by the other climatologies considered, the main exception being the Southern Ocean where it shows a slight heat loss as opposed to the weak heat gain found in the other analyses. In this context, we note that both Solution 3 and GW suggest that the region south of 30^{o} S is an area of weak heat loss to the atmosphere (see Table 4).

The implied Atlantic, Pacific and global ocean heat transports obtained by integrating the surface heat flux fields for each of the various climatologies are shown in Fig.9 together with those for the SOC climatology adjusted according to Solution 3. In the Atlantic, the NCEP/NCAR, Solution 3 and UWM/COADS transports remain in relatively close agreement over a broad range of latitudes while the Trenberth transport is persistently stronger by about 0.2 PW south of 40^{o} N. The higher values for Trenberth reflect the stronger heat loss over the Gulf Stream in the residual analysis. Trenberth is in better agreement with the North Atlantic hydrographic estimates while NCEP/NCAR, Solution 3 and UWM/COADS are closer to hydrography in the mid-latitude South Atlantic. The ECMWF transport is stronger than all of the other climatologies considered in the South Atlantic and is about 0.5 PW higher than the hydrographic estimates. The reason for this difference is that the ECMWF fluxes show a relatively narrow region of heat gain by the ocean in the Tropics (Fig.7) and consequently when they are integrated to form the implied ocean heat transport there is little reduction in its value in the 20^{o} S - 20^{o} N band. Considering the North Pacific, Fig. 9b, the main change from the North Atlantic is that the UWM/COADS transport is now the strongest of those considered. This change reflects the broader area of net heat loss in the North Pacific in UWM/COADS relative to the other analyses (Fig.7).

As regards the global ocean, there is good agreement between the NCEP/NCAR, Solution 3, UWM/COADS and Trenberth transports to about 40^{0}S (particularly so in the 0-40^{0}S band) with some subsequent divergence in the Southern Ocean. The close correspondence between the different climatological values and the hydrographic estimate of the heat transport at 32^{0}S is encouraging. In this context, we note that Trenberth and Caron (2001) have separately found that

the transports from the residually estimated fluxes are in good agreement with values obtained from recent coupled climate models and suggest that convergence towards the true ocean heat transport is now close to being attained. In contrast, the implied ECMWF transport is again significantly different from the other estimates in the Southern Hemisphere with a value at the southern boundary of 0.9 PW which corresponds to a global imbalance of -3 Wm^{-2}. Regional differences between the various climatologies and hydrography are shown in Fig. 10. In the majority of regions considered there is agreement to within 20 Wm^{-2} as was found to be the case for Solution 3. The most noticeable differences are those for the ECMWF fields in the Tropical Atlantic with a bias relative to hydrography of -33 Wm^{-2} in region AT5. The bias again reflects the generally weak heat gain by the ocean in this area in the ECMWF reanalysis.

5. SUMMARY AND DISCUSSION

Results from a linear inverse analysis of the SOC air-sea flux climatology have been presented. The original version of the SOC climatology has a global heat flux bias of 30 Wm^{-2} (Josey et al., 1999) and our aim has been to remove this bias in a manner that is consistent with the improved description of the ocean heat transport that has arisen from WOCE. For our analyses we have used a total of ten constraints distributed throughout the Atlantic and North Pacific oceans. We have examined solutions obtained both with and without the additional requirement of global closure of the ocean heat budget. Without this requirement we obtain a solution (referred to as Solution 1) in which the main adjustments are an increase of 15% to the latent heat flux and reduction of 9% to the shortwave flux. Applying these changes to the SOC climatology we obtain an adjusted set of fields for which the global average net heat flux is -5 Wm^{-2}. This represents a significant improvement on the original gain of 30 Wm^{-2} but is too large an imbalance to be consistent with observed decadal variations in the temperature of the near surface ocean layer which suggest that the global heat budget should close to within about 2 Wm^{-2}.

When the requirement of exact closure of the ocean heat budget is explicitly specified as an additional constraint, the inverse analysis solution obtained (Solution 2) is physically the least reasonable of those considered as it requires a very strong increase in the latent heat flux (25%) and only a minor reduction (2%) to the shortwave. It fails to satisfy the acceptability criterion of Isemer et al. (1989) that the magnitude of each of the free parameter adjustments should be less

than the specified error. It is possible to obtain a solution which satisfies both the Isemer et al. (1989) criterion and the requirement of global closure, if the latter constraint is allowed to have an error of 2 Wm^{-2} that is consistent with the observed decadal temperature variations. In this case, referred to as Solution 3, the adjustments to the four heat flux components are: latent heat (+19%), sensible heat (+7%), longwave (+9%) and shortwave (-6%), and the global mean net heat flux is -2 Wm^{-2}.

Encouraging agreement is obtained between the climatologically implied global ocean heat transport at 32^0 S with Solution 3 and the recent hydrographic estimate at this latitude of Wijffels et al. (2001). In addition, the adjusted SOC fluxes have been compared with other recent climatologies and close agreement found between the implied global ocean heat transport for Solution 3 and independent estimates obtained using residual techniques by Trenberth and Caron (2001) over a broad latitude range. However, comparisons of the adjusted fluxes with research buoy measurements have given more mixed results which suggest that further improvements can be made to our formulation of the inverse analysis problem. In particular, the WHOI FASINEX and Subduction buoy comparisons indicate that the latent heat flux adjustment should have been stronger in the western half of the mid-latitude North Atlantic and weaker in the east.

The interpretation of the parameter adjustments was discussed in Sec 3.3. However, it should be stressed again that the adjustments as defined in our analysis represent the combined error for each flux component arising from the various terms in the flux formulae. Thus, the major adjustment which we have found i.e. the increase in the latent heat flux of 15 or 19% according to Solution 1 or 3, should be interpreted as representing the combination of adjustments to the wind speed, the sea-air humidity difference and the transfer coefficient. It does not represent an adjustment to any one of these terms individually and thus cannot be used as an argument to increase, for example, the value of the transfer coefficient. We note that the uncertainty in any one of these three terms is likely to be of order 10% and thus a combined adjustment of 19%, although large, is not unreasonable.

The inverse analysis has allowed us to obtain a globally balanced set of fluxes from Solution 3, which are consistent with our current hydrographic understanding of ocean heat transport, by means of physically reasonable adjustments to the different heat flux components. In this sense, the adjusted fluxes may be regarded as an improvement on the original SOC

climatology, for which the implied heat transport diverged rapidly from the hydrographic estimates (Fig. 4). Improved agreement with the hydrography is of course to be expected given that the heat transport estimates were used as constraints on the analysis. In order to properly test the adjusted fields it is necessary to carry out comparisons with independent data not used in the analysis. Such data is rather sparse, limiting the number of comparisons that can be carried out. However, the comparisons that we have been able to make with the 32° S and residual method transport estimates have provided positive results (Fig.9c). From these comparisons it appears that the adjusted fields continue to provide a good description of the heat transport when the integration of the climatological net heat flux is extended beyond those regions in which constraints were placed on the analysis.

Despite these encouraging signs, the comparisons with the other independent dataset available to us, namely the WHOI research buoys, raise significant concerns and point to the need for future refinement of our inverse analysis procedure. It should thus be stressed that although we believe the adjusted fields are an improvement on the original SOC climatology, further revisions are likely in the future and thus they should not be used without this caveat in mind. The explicit inclusion of the buoy measurements as constraints in the inverse analysis, together with spatially dependent parameter adjustments, may allow us to resolve the east-west mid-latitude bias found in the North Atlantic and we are currently exploring this possibility. It is likely that regionally varying, rather than globally fixed, parameter adjustments will provide the way forward to further improvements of the SOC climatology using inverse analysis. We also note that thus far we have used inverse analysis parameters which are simple scaling coefficients of each component of the flux. Clearly it will be important to explore other definitions of the parameters, in particular by assigning them to particular variables in the flux formulae, in future analyses.

In addition to the application of inverse methods to constrain the original SOC climatology which has been presented here, separate research is also being carried out into improving our ability to estimate the fluxes. This work is directed both at improving the basic formulae used to estimate the fluxes and increasing the accuracy of ship meteorological reports (Kent, 2002). In particular, recent results have demonstrated that the longwave flux formula used for the original SOC flux climatology was biased by of order 10 Wm^{-2} and a new parameterisation has been developed to resolve this bias (Josey et al., 2003). Research is also being carried out into

the impact of the neglect of aerosol loading in the formula originally used to estimate the shortwave flux fields. Preliminary results from that study indicate that neglect of aerosols can give rise to monthly mean biases of order 20 Wm^{-2} in the Tropics (Grist and Josey, 2003, in preparation). The ultimate goal of this research is the production of a revised version of the SOC climatology, using the new parameterisations and improved corrections, which is globally balanced without the need for heat transport constraints. However, we are still some way from this point and stress that inverse analysis remains an important tool for improving our present estimates of the fluxes.

A key element in the improvement of the SOC flux climatology, and air-sea flux datasets in general, is the evaluation of the flux fields against independent high quality measurements. In practice, this means comparisons against time series from research buoys of the type presented in Section 4.3. At present, the number of such sites is extremely limited and this has prevented assessment of the accuracy of the fluxes in several regions of the global ocean which are potentially essential to understanding why unconstrained flux climatologies fail to close the ocean heat budget. The most noticeable omission is the Southern Ocean, for which it remains unclear whether the ocean gains or loses heat from the atmosphere in the annual mean. Plans for a network of surface flux reference sites are being developed and it is vital that these sites are implemented if further progress is going to be made towards obtaining a reliable picture of the air-sea heat exchange (Send et al., 2001).

Hydrographic estimates of the ocean heat transport are the other key element for evaluation of flux fields. Considerable progress regarding the number and quality of such estimates has been made as a result of WOCE. However, as noted earlier, interpretation of the heat transport values is complicated by variations in the method used to estimate the transport and its error between different studies. These include the choice of reference level velocity for geostrophic calculations, the representation of the heat flux due to eddies and the selection of the wind stress fields used to estimate the Ekman component of the transport. In this context, we note that the adoption of a uniform computational method for the estimation of ocean heat transport from hydrographic observations would facilitate studies such as our own in which these estimates are used to either constrain or evaluate the accuracy of surface flux datasets.

Estimates of the ocean freshwater transport from hydrography provide another potentially useful set of constraints for adjusting flux fields through inverse analysis (e.g. da Silva et al., 1994). We have not employed them in the present study for two main reasons. First, the errors on such estimates are at present uncomfortably large. Second, the use of freshwater constraints requires climatological fields of the precipitation to be included in the inverse analysis and estimates of precipitation from ships remain extremely uncertain (e.g. WGASF, 2000). The development of more accurate precipitation climatologies from satellites may provide a means of making more effective use of freshwater transport estimates in the future to more tightly constrain the adjusted fields.

To summarise, we have used inverse analysis techniques to adjust the SOC climatology in a manner which is consistent with recent estimates of the ocean heat transport and the requirement of global ocean heat budget closure. Good agreement is found between the climatologically implied ocean heat transport obtained from the adjusted fluxes and more recent independent estimates obtained using residual techniques and from hydrography at 32^{o} S. However, comparison of the adjusted fluxes with measurements made by various WHOI research buoys indicates that further improvements to the inverse analysis can still be made to reduce regional biases. We anticipate that subsequent research which incorporates an improved formulation of the inverse analysis parameters will allow the buoy differences to be resolved. Despite these differences we believe that the adjusted fluxes will prove useful, in particular as forcing fields in ocean model studies, and will make them available to interested users.

ACKNOWLEDGEMENTS

The work described in this report has been funded as part of the NERC COAPEC thematic programme under the project: Balancing the Atlantic Heat and Freshwater Budgets, Ref. NER/T/S/2000/00314. We thank Alex Ganachaud, Peter Taylor and the anonymous reviewer for many useful comments. We are also grateful to Bob Weller at WHOI for making available the various research buoy datasets; NCEP, NCAR and ECMWF for the production of their respective reanalysis datasets; Glenn White at NCEP for supplying the NCEP/NCAR fields; Bernard Barnier at LEGI-IMG, Grenoble for the ECMWF fields and Kevin Trenberth at NCAR for the residual analysis fields.

REFERENCES

Aagaard, K. and P. Greisman, 1975: Towards new mass and heat budgets for the Arctic Ocean. *J. Geophys . Res.*, **80**, 3821 - 3827.

Bacon, S, 1997: Circulation and Fluxes in the North Atlantic between Greenland and Ireland. *J. Phys. Oceanogr.*, **27**,1420-1435.

Bryden, H. L, D. H. Roemmich and J. A. Church, 1991: Ocean heat transport across 24^0N in the Pacific. *Deep Sea Res.* **38,** 297-324.

Bryden, H. L, M. A. Griffiths, A. L. Lavin, R. C. Millard, G. Parrilla, and W. M. Smethie 1996: Decadal Changes in Water Mass Characteristics at 24 N in the Subtropical North Atlantic Ocean, *Journal of Climate*, **9** (12), 3162-3186.

Bryden, H. L. and S. Imawaki, 2001: Ocean Heat Transport. Chapter in : *Ocean Circulation and Climate*, G. Siedler, J. Church and J. Gould, Ed., Academic Press, 455-474.

Clark, N. E., L. Eber, R. M. Laurs, J. A. Renner, and J. F. T. Saur, 1974: Heat exchange between ocean and atmosphere in the eastern North Pacific for 1961 - 71. *NOAA Tech. Rep. NMFS SSRF-682***,** 108.

Cressman, G. P., 1959: An operational objective analysis scheme. Mon. Wea. Rev., **87**, 329 - 340.

da Silva, A. M., C. C. Young and S. Levitus, 1994: Atlas of Surface Marine Data Vol. 1: Algorithms and Procedures. *NOAA Atlas series*, pp.74.

Fairall, C. W., E. F. Bradley, D. P. Rogers, J. B. Edson, and G. S. Young, 1996: Bulk parameterization of air-sea fluxes for TOGA-COARE. *J. Geophys. Res.*, **101,** 3747 - 3764.

Friederichs, M. A. M. and M. M. Hall, 1993: Deep circulation in the tropical North Atlantic. *J. Marine Res.*, **52,** 583-638.

Ganachaud, A. and C. Wunsch, 2000: Improved estimates of global ocean circulation, heat transport and mixing from hydrographic data. *Nature*, **408,** 453-457.

Gleckler, P. J. and B. C. Weare, 1997: Uncertainties in global ocean surface heat flux climatologies derived from ship observations. J. Clim., **10**(11), 2764 - 2781.

Grist, J. P. and Josey, S. A., 2002: Balancing the SOC climatology using inverse analysis with spatially fixed parameter adjustments, Southampton Oceanography Centre Internal Document No. 80, Southampton, 38 pp. + figs.

Hellerman, S. and M. Rosenstein, 1983: Normal monthly wind stress over the World Ocean with error estimates. *J. Phys. Oceanogr.*, **13,** 1093 - 1104.

Holfort, J. and G. Siedler, 2001: The meridional oceanic transports of heat and nutrients in the South Atlantic. *J. Phys. Oceanogr.*, **31**, 5-29.

Isemer, H.-J. and L. Hasse, 1987: *The Bunker climate atlas of the North Atlantic Ocean. Vol.2: Air-sea interactions. Springer-Verlag*, Springer-Verlag, 252 pp

Isemer, H.-J., J. Willebrand and L. Hasse, 1989: Fine adjustment of large scale air-sea energy flux parameterizations by direct estimates of ocean heat transport. *J. Clim.*, **2**, 1173 - 1184.

Josey, S. A., E. C. Kent and P. K. Taylor, 1998: The Southampton Oceanography Centre (SOC) Ocean - Atmosphere Heat, Momentum and Freshwater Flux Atlas. *Southampton Oceanography Centre Report No. 6, Southampton, UK*, 30 pp. & figs.

Josey, S. A., E. C. Kent and P. K. Taylor, 1999: New insights into the ocean heat budget closure problem from analysis of the SOC air-sea flux climatology. *J. Climate*, **12**(9), 2856 - 2880.

Josey, S. A., E. C. Kent, and P. K. Taylor, 2002: On the Wind Stress Forcing of the Ocean in the SOC Climatology: Comparisons with the NCEP/NCAR, ECMWF, UWM/COADS and Hellerman and Rosenstein Datasets. *Journal of Physical Oceanography*, **32,** 1993 - 2019.

Josey, S. A., 2001: A Comparison of ECMWF, NCEP/NCAR and SOC Surface Heat Fluxes with Moored Buoy Measurements In The Subduction Region of the North-East Atlantic. Journal of Climate, **14**(8), 1780-1789.

Josey, S. A., R. W. Pascal, P. K. Taylor and M. J. Yelland, 2003: A New Formula For Determining the Atmospheric Longwave Flux at the Ocean Surface at Mid-High Latitudes. *J. Geophys. Res.*, in press.

Kallberg, P., 1997: *ECMWF Re-Analysis Project Report Series Part 2: Aspects of the re-analysed climate*, ECMWF, Reading, UK, pp. 89.

Kalnay, E., M. Kanamitsu, R. Kistler, W. Collins, D. Deaven, L. Gandin, M. Iredell, S. Saha, G. White, J. Woollen, Y. Zhu, A. Leetmaa, R. Reynolds, M. Chelliah, W. Ebisuzaki, W.Higgins, J. Janowiak, K. C. Mo, C. Ropelewski, J. Wang, R. Jenne and D. Joseph, 1996: The NCEP/NCAR 40-Year Reanalysis Project. Bulletin of the American Meteorological Society, 77(3), 437-471.

Kent, E. C., 2002: Assessment of Biases in Merchant Ship Surface Temperatures. SOC Research and Consultancy Report No. 58 to Hadley Centre for Climate Prediction and Research and DEFRA, March 2002, 97pp.

Kent, E. C., P. G. Challenor, and P. K. Taylor, 1999: A statistical determination of the random observational errors present in voluntary observing ships meteorological reports. *J. Atmos. Ocean. Tech.*, **16,** 905 - 914.

Kent, E. C., P. K. Taylor, B. S. Truscott and J. S. Hopkins, 1993a: The accuracy of voluntary observing ships meteorological observations - results of the VSOP - NA. *J. Atmos. & Oceanic Tech.*, **10**(4), 591 - 608.

Kent, E. C., R. J. Tiddy and P. K. Taylor, 1993b: Correction of marine air temperature observations for solar radiation effects. *J. Atmos. & Oceanic Tech.*, **10**(6), 900 - 906.

Klein, B., R. L. Molinari, T. J. Mueller and G. Siedler, 1995: A transatlantic section at 14.5 N : Meridional volume and heat fluxes. *J. Mar. Res.*, **53**, 929 - 957.

Koltermann, K. P., A. V. Sokov, V. P. Tereschenkov, S. A. Dobroliubov, K. Lorbacher, and A. Sy, 1999: Decadal changes in the thermohaline circulation of the North Atlantic. *Deep-Sea Res. II*, **46,** 109 - 138.

Lavin, A., H. L. Bryden, and G. Parrilla, 1998: Meridional transport and heat flux variations in the subtropical North Atlantic. *The Global Atmosphere and Ocean System*, **6,** 269-293

Macdonald, A., J. Candela, and H. L. Bryden, 1994: An estimate of the net heat transport through the Strait of Gibraltar. In: La Violette, P. E. (Ed.), *Coastal Estuarine Studies*, **46,** 13-32, AGU, Washington, D. C.

Menke, W., 1984: Geophysical Data Analysis: Discrete Inverse Theory. Academic Press, 257 pp.

Moyer, K. A. and R. A. Weller, 1997: Observations of surface forcing from the Subduction Experiment : a comparison with global model products and climatological data sets. J. Clim., **10**(11), 2725 - 2742.

Oberhuber, J. M., 1988: An atlas based on the COADS data set : the budgets of heat, buoyancy and turbulent kinetic energy at the surface of the global ocean. MPI Report, **15,** 19 pp.

Payne, R. E., 1972: Albedo of the sea surface. *J. Atmos. Sci.*, **29,** 959 - 970.

Reed, R. K., 1977: On estimating insolation over the ocean. *J. Phys. Oceanogr.*, **7,** 482-485.

Roemmich, D. and McCallister, T, 1989: Large scale circulation of the north Pacific. *Prog. Oceanogr,* **22**, 171-204.

Saunders, P. M. and B. A. King, 1995: Oceanic fluxes on the WOCE A11 section. *J. Phys. Oceanogr.*, **25**, 1942-1958.

Send, U., R. Weller, S. Cunningham, C. Eriksen, T. Dickey, M. Kawabe, R. Lukas, M. McCartney, and S. Østerhus, 2001: Oceanographic Timeseries Observatories. *Observing the Oceans in the 21st Century*, C.J.Koblinsky and N.R.Smith, Eds., GODAE Project Office and the Bureau of Meteorology, 376-390.

Speer, K. G, J. Holfort, T. Reynaud, G. Siedler, 1996: South Atlantic heat Transport at 11S. *The South Atlantic: Present and Past circulation.* Springer, Berlin.

Tragou, E., C. Garrett and R. Outerbridge, 1999: The heat and freshwater budgets of the Red Sea. *J. Phys. Oceanogr.*, **29**(10), 2504 - 2522.

Trenberth, K. E. and J. M. Caron, 2001: Estimates of meridional atmosphere and ocean heat transports. *J. Climate*, **14,** 3433-3443.

Trenberth, K. E., J. M. Caron, and D. P. Stepaniak, 2001: The atmospheric energy budget and implications for surface fluxes and ocean heat transports. *Clim. Dyn.*, **17,** 259-276.

WGASF, 2000: Intercomparison and Validation of Ocean-Atmosphere Energy Flux Fields - *Final report of the Joint WCRP/SCOR Working Group on Air-Sea Fluxes* (P. K. Taylor, ed.) November 2000, WCRP-112 (WMO/TD-No. 1036), 306 pp.

Weller, R. A., M. F. Baumgartner, S. A. Josey, A. S. Fischer, and J. Kindle, 1998: Atmospheric forcing in the Arabian Sea during 1994-1995: observations and comparisons with climatology and models. Deep Sea Research, **45**, 11, 1961 -1999.

Wijffels, S. E., J. M. Toole, H. L. Bryden, R. A. Fine, W. J. Jenkins, and J. L. Bullister, 1996: The water masses and circulation at 10 N in the Pacific. *Deep-Sea Research*, **1,** 501 - 544.

Wijffels, S. E., J. M. Toole, and R. Davis, 2001: Revisiting the South Pacific subtropical circulation: A synthesis of World Ocean Circulation Experiment Observations along 32º S. *J. Geophys. Res.*, **106,** 19,481-19,513.

WMO, 1993: International list of selected, supplementary and auxiliary ships. WMO Report, WMO, Geneva, various pagination.

Woodruff, S. D., S. J. Lubker, K. Wolter, S. J. Worley and J. D. Elms, 1993: Comprehensive Ocean-Atmosphere Data Set (COADS) release 1a: 1980-92. *Earth System Monitor*, **4**(1), 4-8.

TABLES

Section	Constraint Number	Heat transport (PW)	Reference
CONVEX Atlantic	1	0.28 ± 0.06	Bacon (1997)
24^0 N Atlantic	2	1.22 ± 0.30	Hall and Bryden (1982)
14^0 N Atlantic	3	1.22 ± 0.42	Klein et al (1995)
8^0 N Atlantic	4	1.18 ± 0.52	Klein et al (1995)
11^0 S Atlantic	5	0.60 ± 0.17	Speer et al (1996)
30^0 S Atlantic	6	0.29 ± 0.29	Holfort and Siedler (2001)
A11 Atlantic	7	0.46 ± 0.16	McDonagh, E., personal comm.*
46^0 N Pacific	8	-0.09 ± 0.30	Roemmich and McCallister (1989)
24^0 N Pacific	9	0.76 ± 0.30	Bryden et al (1991)
10^0 N Pacific	10	0.70 ± 0.50	Wijffels et al.(1996)
65^0 N Atlantic	Northern Reference	0.1 (exact)	Aagard and Greisman (1975)
66^0 N Pacific	Northern Reference	0.002 (exact)	Aagard and Greisman (1975)

Table 1. Hydrographic measurements of the heat transport used for the inverse analysis, the error estimates have been taken from the original reference in each case. * Note the A11 value has been obtained from a recent reworking of the hydrographic section described originally by Saunders and King (1995).

Solution	x_E	x_H	x_L	x_S
Solution 1 - No Global Closure	0.15	0.06	0.09	-0.09
Solution 2 - Exact Global Closure	0.25	0.09	0.08	-0.02
Solution 3 - Global Closure to ± 2 Wm^{-2}	0.19	0.07	0.09	-0.06

Table 2. Fractional adjustments to the inverse analysis parameters for the three solutions described in the text. Each solution has been obtained using all ten heat transport constraints and $e_E=e_H=e_L=e_S=0.2$. The additional constraint of global closure has been applied as indicated in the first column.

Solution	Q_E	Q_H	Q_L	Q_S	Q_N
Original SOC	-90	-7	-49	176	30
Adjusted SOC (Solution 1)	-104	-8	-53	160	-5
Adjusted SOC (Solution 2)	-112	-8	-53	173	0
Adjusted SOC (Solution 3)	-107	-8	-53	166	-2

Table 3. Values for the global mean air-sea heat flux components and the net heat flux from the original SOC climatology and the SOC climatology adjusted according to the three inverse analysis solutions.

Region	Area Averaged Net Heat Flux (Wm^{-2})				
	Ganachaud	SOC	Solution 1	Solution 2	Solution 3
N of 47° N	-39±7	-17 ± 4	-37± 4	-36±5	-37±5
24° - 47° N	-24±4	9±4	-25±4	-22±4	-24±4
30° S - 24° N	13±2	50±8	9± 8	14±9	11±9
S of 30° S	-8±3	12± 8	-14± 9	-10±10	-12± 9

Table 4. Area averaged values of the net air-sea heat flux in various latitude bands from Ganachaud and Wunsch (2000), the unadjusted SOC climatology and the SOC climatology adjusted according to the three inverse analysis solutions described in the text. Error values for the SOC fluxes are the standard deviation of the sample of 14 individual yearly mean values which is taken as an upper limit for the random error.

Section	Heat transport (PW)	Reference
46° N	0.49 ± 0.23	*Koltermann et al. (1999) (Atlantic) Roemmich and McCallister (1989) (Pacific)
24° N	1.98 ± 0.42	Hall and Bryden (1982) (Atlantic) Bryden et al (1991) (Pacific)
10° N	1.80 ± 0.56	Wijffels et al.1996a (Pacific) *Freidrichs and Hall (1993) (Atlantic)
30 ° S	-0.46±38	Holfort and Siedler (2001) (Atlantic) *Wijffels et al (2001) (Indo-Pacific)

Table 5. Hydrographic estimates of the global ocean heat transport obtained by combining values at the same latitude in different basins from the listed references. The heat transport estimates from those references marked with a * were not employed in the inverse analysis.

Subduction Array (18-33° N, 22-34° W)

	Latent	Sensible	Shortwave	Longwave	Net
Buoy	-103	-7	209	-62	37
SOC	-108	-7	200	-56	29
(SOC - buoy)	(-5)	(0)	(-9)	(6)	(-8)
S3	-129	-7	189	-61	-8
(S3 - buoy)	(-26)	(0)	(-20)	(1)	(-45)

Table 6a. Deployment average values of the various heat flux components and the net heat flux for the Subduction Array (Buoy), the original SOC climatology (SOC) and the climatology adjusted according to Solution 3 (S3).

Arabian Sea Buoy (15.5°N, 61.5°E)

	Latent	Sensible	Shortwave	Longwave	Net
Buoy	-121	-2	243	-59	61
SOC	-110	-1	240	-51	78
(SOC - buoy)	(11)	(1)	(-3)	(8)	(17)
S3	-131	-1	226	-56	38
(S3 - buoy)	(-20)	(1)	(-17)	(3)	(-23)

Table 6b. Deployment average values of the various heat flux components and the net heat flux for the Arabian Sea buoy (Buoy), the original SOC climatology (SOC) and the climatology adjusted according to Solution 3 (S3).

TOGA-COARE buoy (1.75°S, 156°E)

	Latent	Sensible	Shortwave	Longwave	Net
Buoy	-108	-9	196	-58	21
SOC	-115	-10	219	-50	44
(SOC - buoy)	(-7)	(-1)	(23)	(8)	(23)
S3	-136	-10	208	-54	8
(S3 - buoy)	(-28)	(-1)	(12)	(4)	(-13)

Table 6c. Deployment average values of the various heat flux components and the net heat flux for the TOGA-COARE buoy (Buoy), the original SOC climatology (SOC) and the climatology adjusted according to Solution 3 (S3).

FASINEX array (27°N, 70°W)

	Latent	Sensible	Shortwave	Longwave	Latent + Sensible + Shortwave
Buoy	-170	-17	222	---	35
SOC	-125	-10	220	-63	85
(SOC - buoy)	(45)	(7)	(-2)	(---)	(50)
S3	-149	-11	208	-69	48
(S3 - buoy)	(21)	(6)	(-14)	(---)	(13)

Table 6d. Deployment average values of the various heat flux components and the net heat flux for the FASINEX Array (Buoy), the original SOC climatology (SOC) and the climatology adjusted according to Solution 3 (S3). Note that longwave measurements were not made on this deployment and that the final column shows the sum of the latent, sensible and shortwave fluxes.

FIGURE CAPTIONS

Figure 1. a.) Map showing the locations of the hydrographic sections (solid lines) for which estimates of the ocean heat transport were used as constraints or reference values in the study. The regions between the hydrographic sections are labelled for ease of reference e.g. AT1. Note that the dashed line at 32° S indicates an additional section used in the evaluation of the analysis solutions. b.) Distribution with time of the hydrographic sections. Crosses indicate individual sections which are labelled according to latitude (except for the non-zonal CONVEX and A11 sections) and the relevant ocean basin as follows Atlantic (At), Pacific (Pa) and Indian (In). The solid bar represents the period spanned by the SOC climatology. Note that for ease of presentation we have shown the 1982 section across 24°N rather than the 1957 section analysed by Hall and Bryden (1982) which was the source of our heat transport constraint at this latitude; the two sections provide very similar values for the heat transport.

Figure 2. Annual mean net heat flux field for a.) the SOC climatology, and b.) the SOC climatology adjusted according to Solution 1, c.) Solution 2 and d.) Solution 3. Contour intervals are 50 Wm^{-2}, negative heat flux (i.e. heat loss to the atmosphere) is shaded grey.

Figure 3 The difference (adjusted-original) between the adjusted field and the SOC climatology for a.) Solution 1; b) Solution 2 and c.) Solution 3. Contour intervals are 10 Wm^{-2}, values less than -30 Wm^{-2} are shaded grey.

Figure 4. Climatologically implied ocean heat transport for a) the Atlantic Ocean, b) the Pacific Ocean and c) the Global Ocean for the original SOC climatology (solid grey line), Solution 1 (dot-dashed line), Solution 2 (dashed line) and Solution 3 (solid black line). Crosses indicate hydrographic estimates of the heat transport.

Figure 5. The difference (climatology-hydrography) between area averaged net heat flux values from the SOC climatology and hydrography for a.) the original SOC climatology ; b.) the SOC climatology adjusted according to Solution 1; c) the SOC climatology adjusted according to Solution 2 and d.) the SOC climatology adjusted according to Solution 3 (units Wm^{-2}).

Figure 6. Summary plot showing the difference (ΔQ) between SOC estimates and WHOI research buoy measurements of the heat flux components and the net heat flux for various buoy deployments. Black bars : differences between the original SOC climatology and the buoys. Grey bars : differences between adjusted SOC Solution 3 and the buoys. The abbreviations refer to the different buoys considered as follows: Sub. - Mean of Subduction buoy array; A. Sea - Arabian Sea Buoy; TOGA - TOGA-COARE buoy; FAS. - Mean of FASINEX buoy array. Note that buoy measurements of the longwave were not available for FASINEX and that in this case the net heat flux differences are an approximation based on the sum of the latent, sensible and shortwave fluxes.

Figure 7. Climatological annual mean net heat flux for a.) Trenberth residual ; b.) NCEP reanalysis; c.) ECMWF reanalysis and d.) UWM/COADS (adjusted). Contour intervals are 50 Wm^{-2}, negative heat flux (i.e. heat loss to the atmosphere) is shaded grey.

Figure 8. Zonally averaged annual mean net heat flux for the SOC climatology adjusted according to Solution 3 (solid black line), UWM/COADS (adjusted) (solid grey line), Trenberth residual (dashed black line), NCEP reanalysis (dashed grey line) and ECMWF reanalysis (black dot-dashed line).

Figure 9 Ocean heat transport as calculated from various climatologies: adjusted SOC solution 3 (solid black line), UWM/COADS (adjusted) (solid grey line), Trenberth residual (dashed black line), NCEP reanalysis (dashed grey line) and ECMWF reanalysis (black dot-dashed line), for a) the Atlantic ocean, b) the Pacific ocean and c) the Global ocean. Crosses indicate hydrographic estimates of the heat transport.

Figure 10. The difference (climatology-hydrography) between area averaged net heat flux values from various climatologies and hydrography for a) Trenberth residual, b) NCEP reanalysis, c) ECMWF reanalysis and d) UWM/COADS (adjusted), units Wm^{-2}.

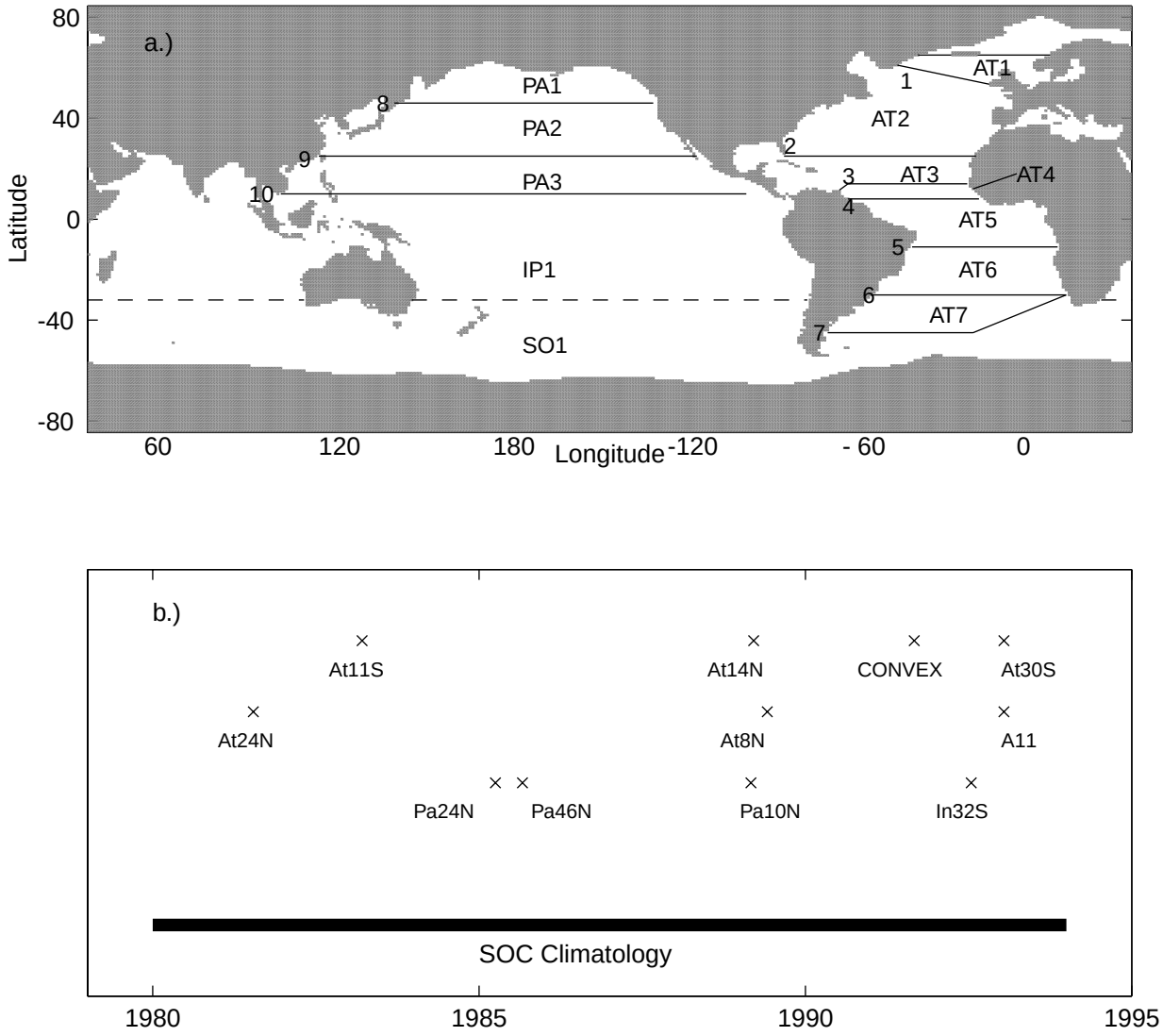

Fig. 1 a.) Map showing the locations of the hydrographic sections (solid lines) for which estimates of the ocean heat transport were used as constraints or reference values in the study. The regions between the hydrographic sections are labelled for ease of reference e.g. AT1. Note that the dashed line at 32^{o} S indicates an additional section used in the evaluation of the analysis solutions; b.) Distribution with time of the hydrographic sections. Crosses indicate individual sections which are labelled according to latitude (except for the nonzonal CONVEX and A11 sections) and the relevant ocean basin as follows Atlantic (At), Pacific (Pa), Indian (In). The solid bar represents the period spanned by the SOC climatology.

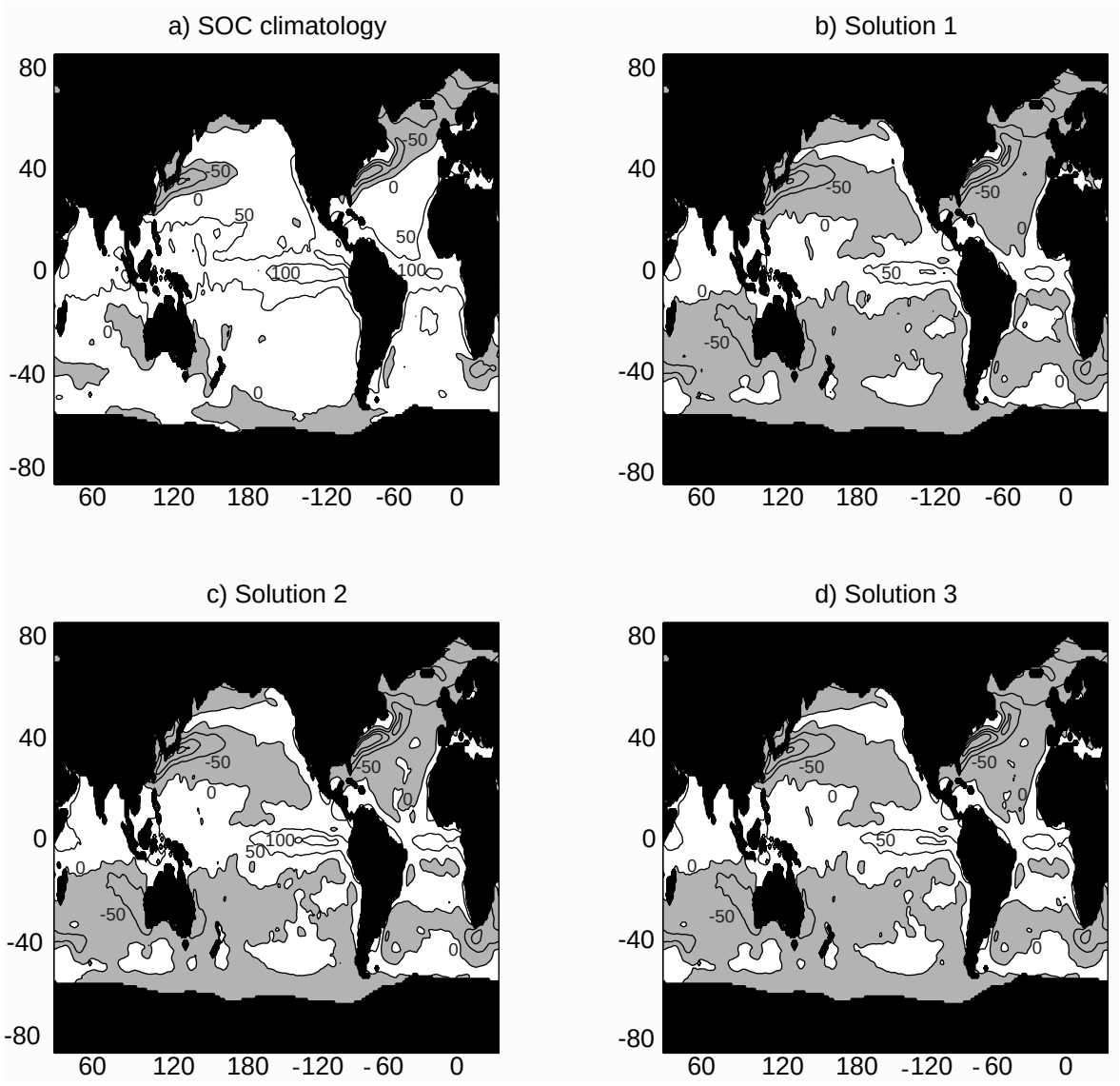

Fig. 2. Annual mean net heat flux field for a.) the SOC climatology, and b.) the SOC climatology adjusted according to Solution 1, c.) Solution 2 and d.) Solution 3. Contour intervals are 50 Wm^{-2}, negative heat flux (i.e. heat loss to atmosphere) is shaded grey.

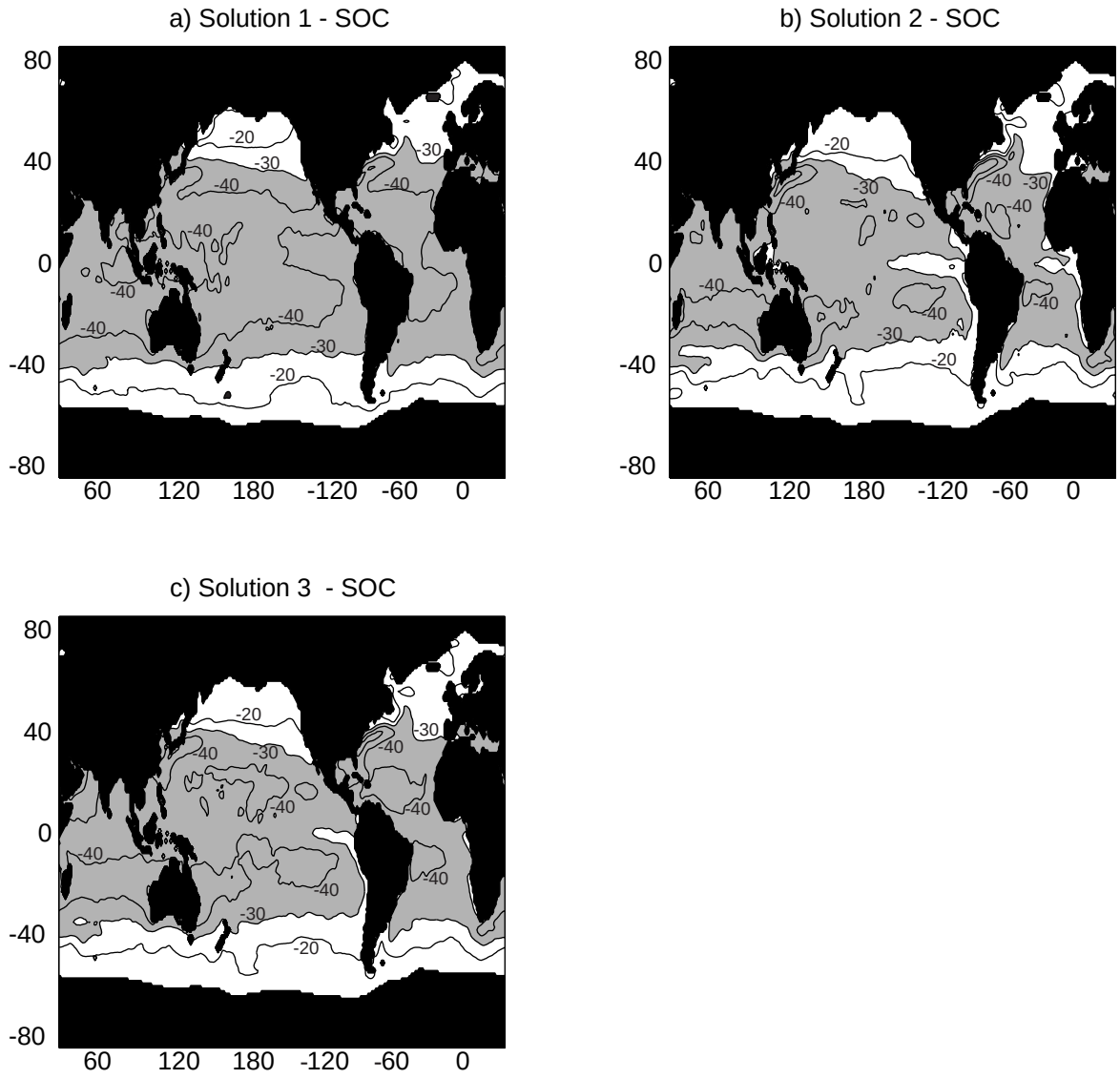

Figure 3 The difference (adjusted-original) between the adjusted field and the SOC climatology for a.) Solution 1; b) Solution 2 and c.) Solution 3. Contours are every 10 Wm^{-2}, values less than -30 Wm^{-2} are shaded grey.

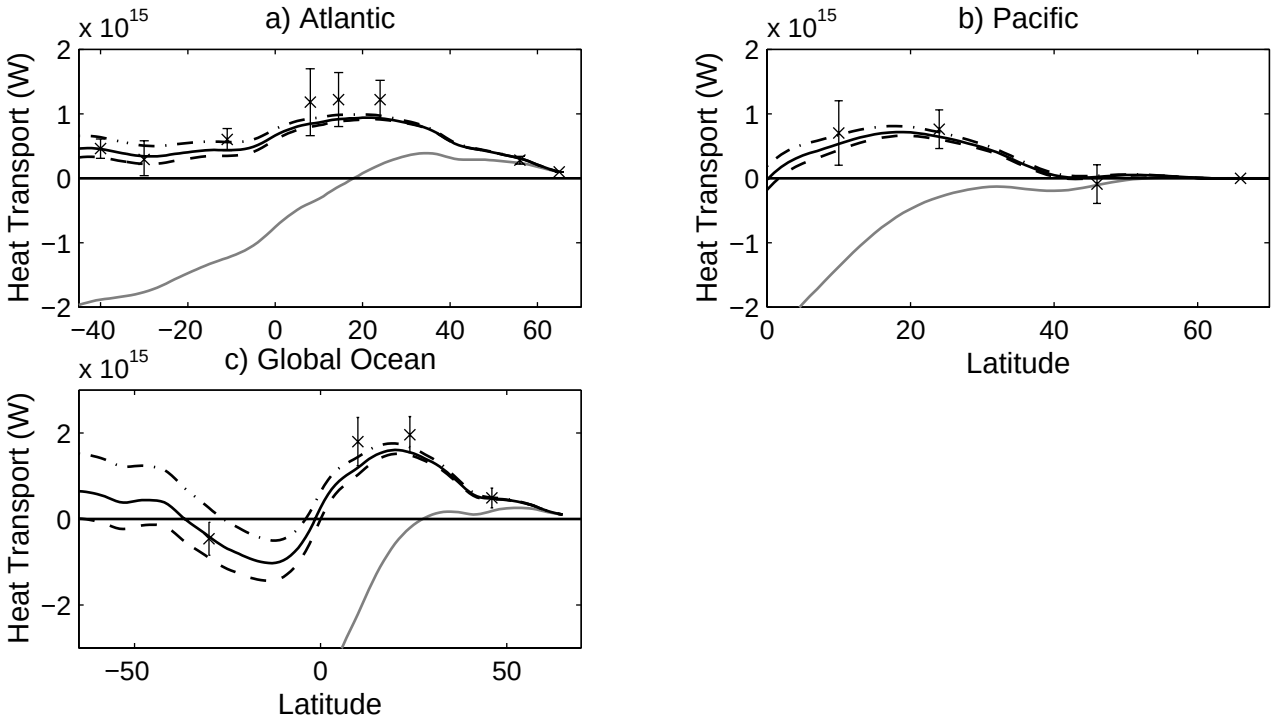

Fig. 4. Climatologically implied ocean heat transport for a) the Alantic Ocean, b) the Pacific Ocean and c) the Global Ocean for the original SOC climatology (solid grey line), Solution 1 (dot−dashed line), Solution 2 (dashed line) and Solution 3 (solid black line). Crosses indicate hydrographic estimates of the heat transport.

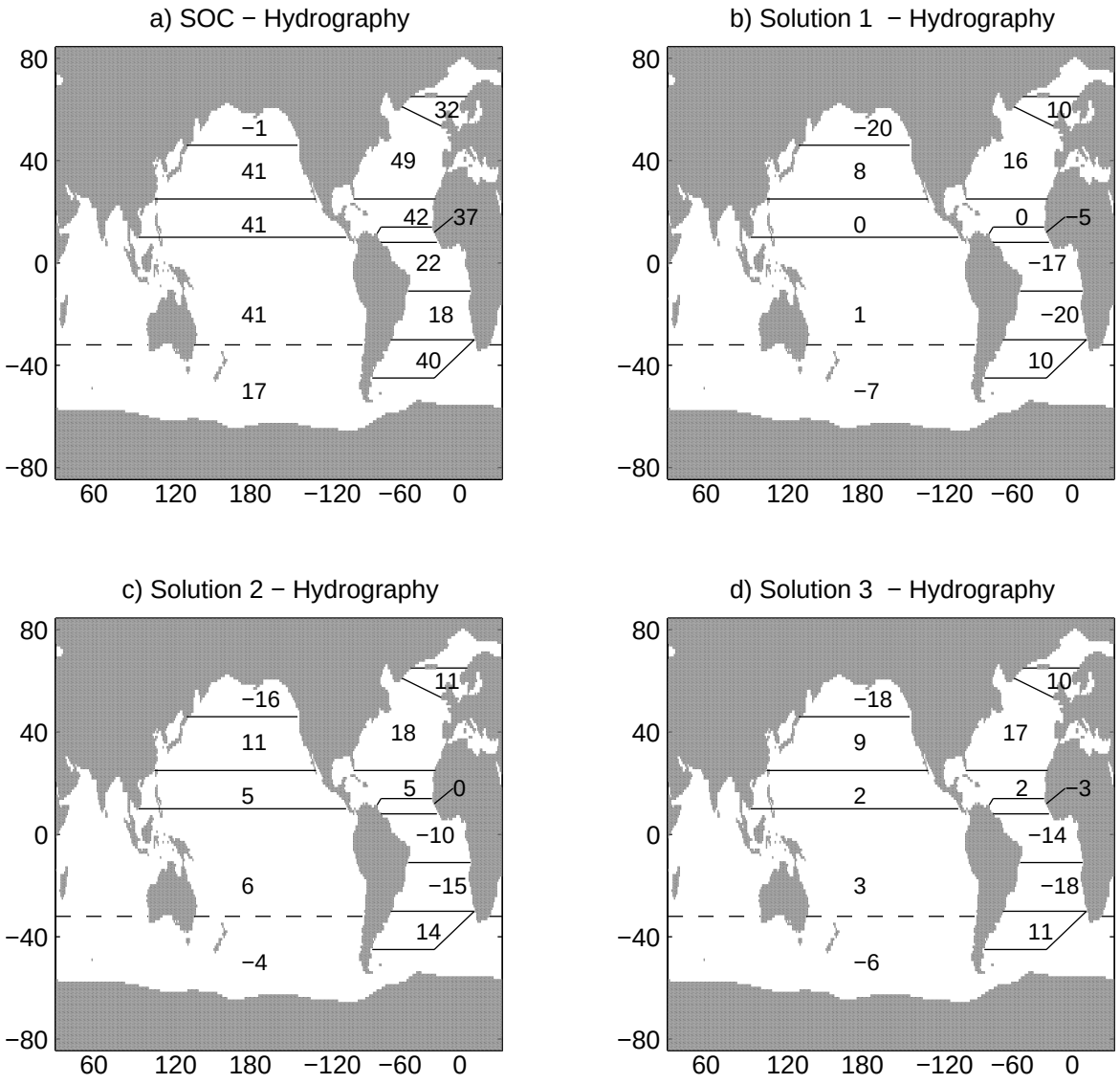

Fig. 5. Difference (climatology−hydrography) between the area averaged heat flux from the SOC climatology and hydrography for a) the original SOC climatology; b.) the SOC climatology adjusted according to Solution 1; c) the SOC climatology adjusted according to Solution 2 and d.) the SOC climatology adjusted according to Solution 3 (units Wm^{-2}).

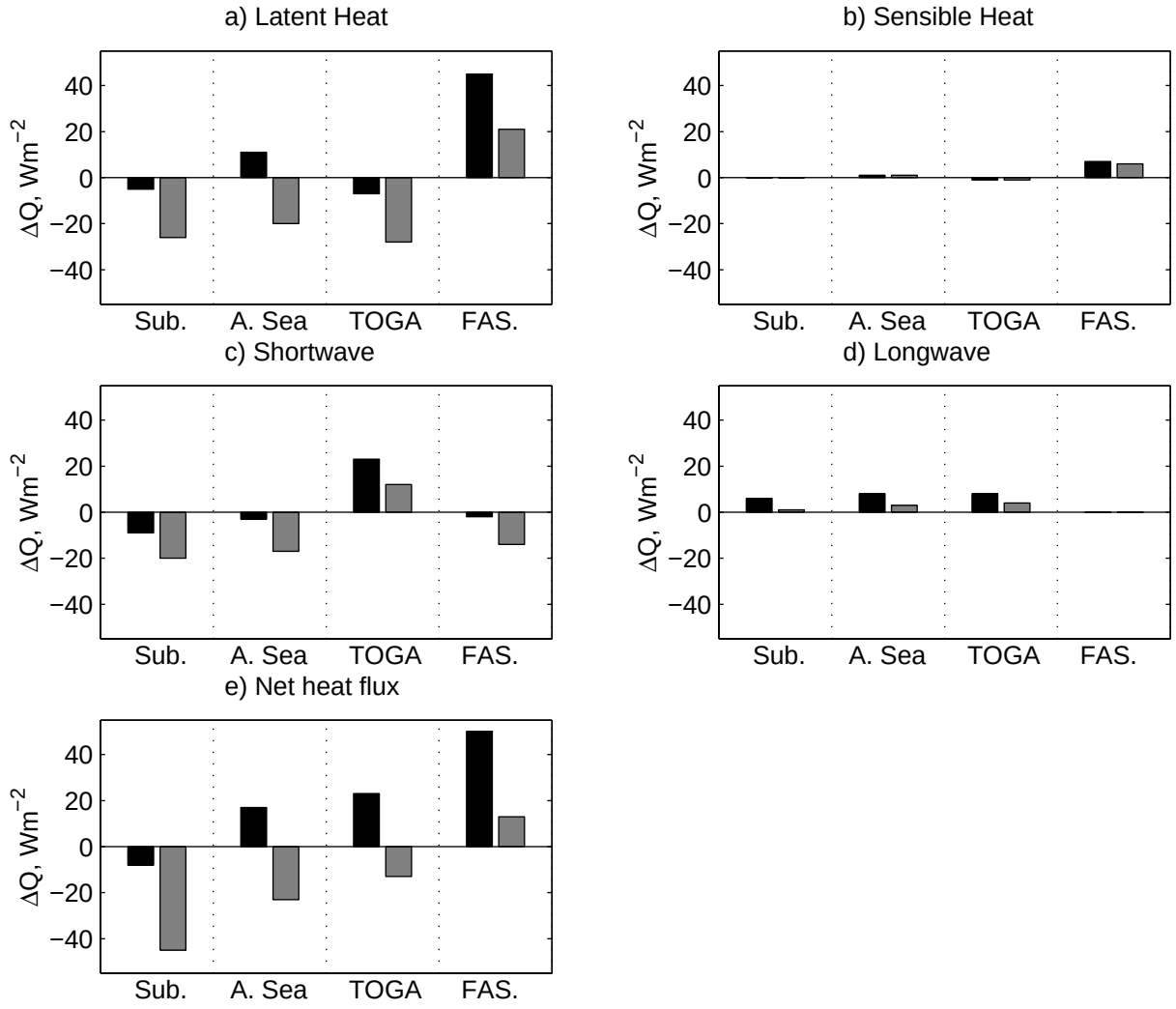

Fig. 6. Summary plot showing the difference (ΔQ) between SOC estimates and WHOI research buoy measurements of the heat flux components and the net heat flux for various buoy deployments. Black bars: differences between the original SOC climatology and the buoys. Grey bars: differences between adjusted SOC Solution 3 and the buoys. The abbreviations refer to the different buoys considered as follows: Sub. Mean of Subduction buoy array; A. Sea − Arabian Sea Buoy; TOGA − TOGA−COARE Buoy; FAS. − Mean of FASINEX Buoy array. Note that buoy measurements of the longwave were not available for FASINEX and that in this case the net heat flux differences are an approximation based on the sum of latent, sensible and shortwave fluxes.

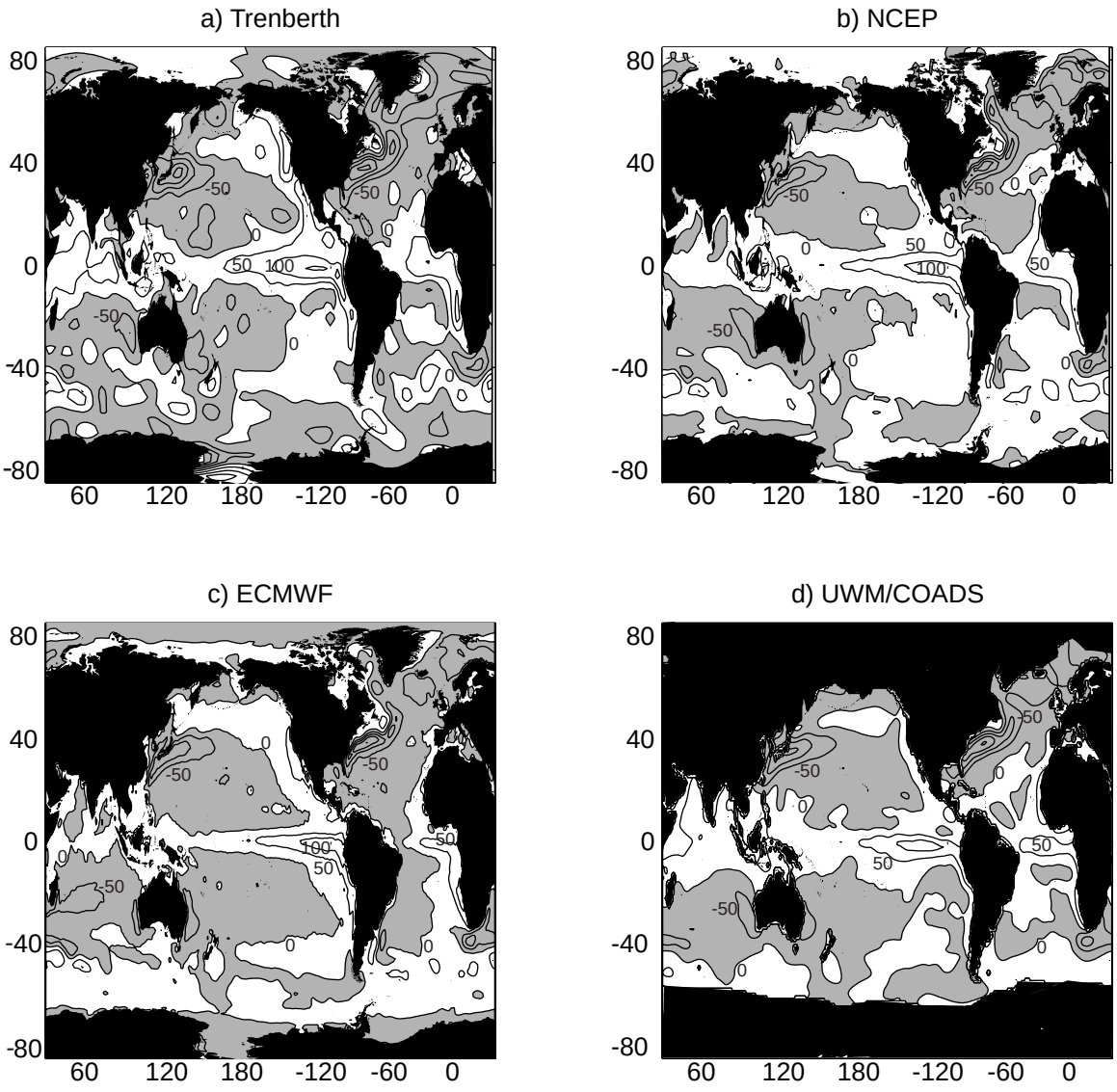

Figure 7 Climatological annual mean net heat flux for a.) Trenberth residual; b) NCEP reanalysis; c) ECMWF reanalysis and d.) UWM/COADS (adjusted). Contour intervals are 50Wm^{-2}, negative heat flux (i.e. heat loss to atmosphere) is shaded grey.

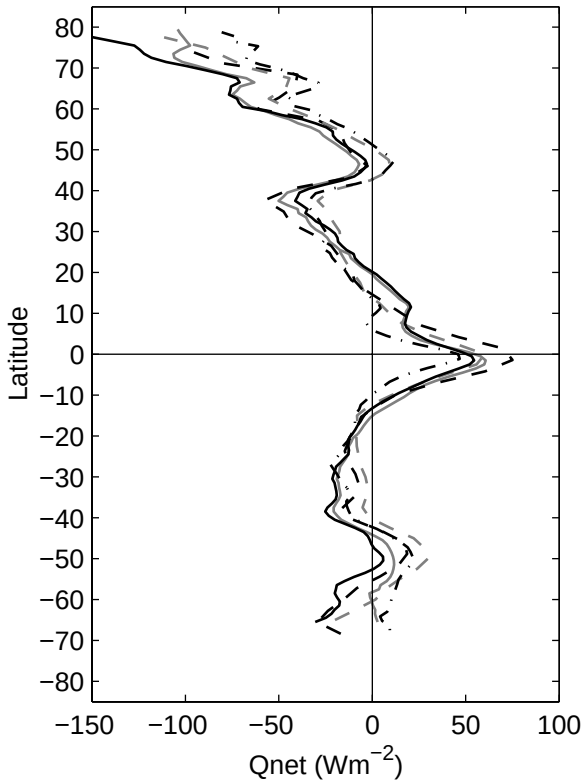

Fig. 8. Zonally averaged annual mean net heat flux for the SOC climatology adjusted according to Solution 3 (solid black line), UWM/COADS (adjusted) (solid grey line), Trenberth residual (dashed black line), NCEP reanalysis (dashed grey line), and ECMWF reanalysis (black dot−dashed line).

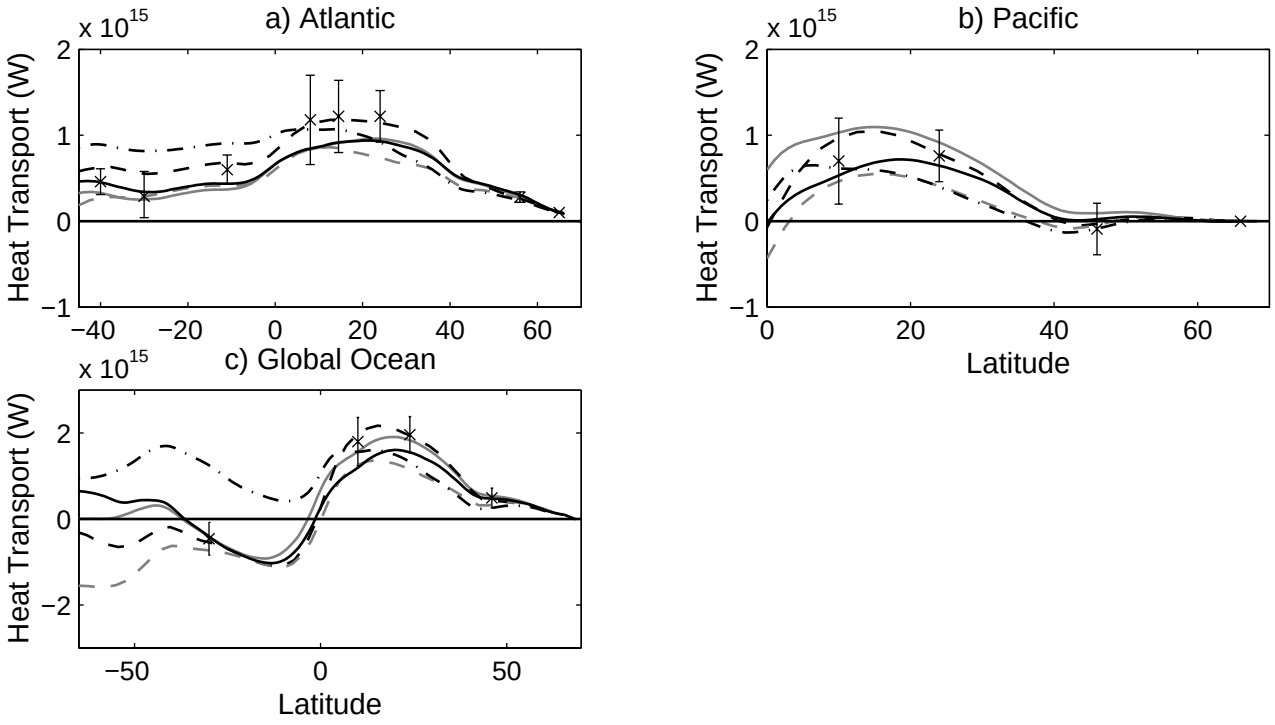

Fig. 9. Ocean heat transport as calculated from various climatologies: adjusted SOC solution 3 (solid black line), UWM/COADS (adjusted) (solid grey line), Trenberth residual (dashed black line), NCEP reanalysis (dashed grey line) and ECMWF reanalysis (black dot−dashed line), for a) Atlantic ocean, b) the Pacific ocean, and c) the Global ocean. Crosses indicate hydrographic estimates of the heat transport.

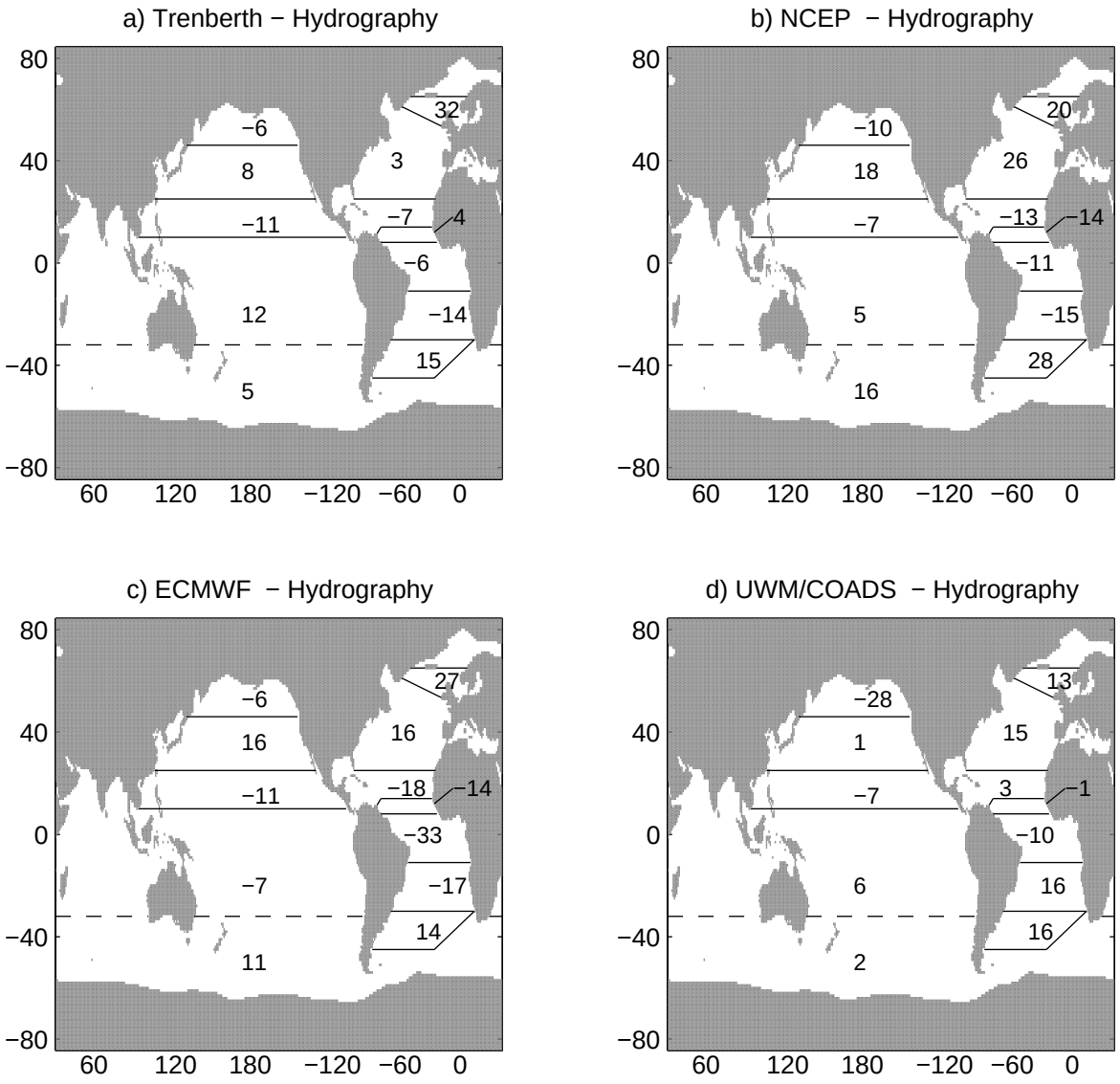

Fig. 10. The difference (climatology−hydrography) between the area averaged heat flux from various climatologies and hydrography for a) Trenberth residual, b) NCEP reanalysis c) ECMWF reanalysis, and d) UWM/COADS (adjusted) (units Wm^{-2}).